Electronic Supplementary Information

Design and Facile Synthesis of Photothermally Active Metal-Organic Framework Bearing Persistent Radicals *via* Post-synthetic Thermal Annealing

Yuan-Hui Zhong,[a,b] Lai-Hon Chung,[a]* Sheng-Yi Zhao,[a] Zihao Feng,[a] Jieying Hu,[a] Ning Li,[a] Wei-Ming Liao,[a] Wai-Yeung Wong,[b] Lin Yu,[a] and Jun He[a]*

[a] School of Chemical Engineering and Light Industry, Guangdong University of Technology, Guangzhou 510006, China

[b] Department of Applied Biology and Chemical Technology, The Hong Kong Polytechnic University (PolyU), Hung Hom, Hong Kong, PR China

Table of contents

General procedure

Materials and characterization

Starting materials, reagents, and solvents were purchased from commercial sources (J&K, Zhengzhou Alfa and Acros) and used without further purification. Elemental analysis was obtained with a VarioMicro CUBE CHN elemental analyzer. Powder X-ray diffraction (PXRD) patterns were collected on a Rigaku Smart lab diffractometer with Cu Kα radiation (λ = 1.5418 Å) at room temperature. The X-ray tube operated at a voltage of 40 kV and a current of 15 mA. Fourier transform infrared (FT-IR) spectra in the range 400–4000 cm^{-1} were recorded on a Nicolet Avatar 360 FT-IR spectrophotometer. Solution ^{1}H NMR and ^{13}C NMR spectra were recorded on a 400 MHz Bruker superconducting magnet high-field Nuclear Magnetic Resonance (NMR) spectrometer at 298 K, with tetramethylsilane (TMS) as the internal standard. Chemical shifts (δ) are expressed in ppm relative to the residual solvent (*e.g.*, $CDCl_3$ ^{1}H: 7.26 ppm, ^{13}C: 77.16 ppm) reference. Coupling constants are expressed in hertz. Thermogravimetric analysis (TGA) was carried out in a PerkinElmer thermal analysis equipment (STA 6000) with a heating rate of 5 °C/minute. Diffuse reflection spectra were collected in the UV-Visible Near Infra-Red Spectrophotometer with Integrating Sphere (Shimazu 3600 plus). The fluorescence spectra were measured using HORIBA Scientific Fluorolog-3 at room temperature. The porosity and surface area analysis were performed using a Quantachrome Autosorb iQ gas sorption analyzer. The sample was outgassed at 0.03 torr with a 5 °C /minute ramp to 110 °C and held at these temperatures for 12 hours. transmission electron microscope (TEM) images were obtained from a field-emission transmission electron microscope (Hitachi, SU8220). All of the magnetic data was obtained from a physical property measurement system (PPMS, DynaCool, Quantum Design Inc.). The electron paramagnetic resonance (EPR) spectra were recorded using a Bruker ER-420 spectrometer. The central magnetic field was 3350 G, and the modulation frequency was 100 kHz.

The variable-temperature EPR data in solid state were fitted by modified Bleaney-Bowers equation to calculate singlet-triplet gap:

$$IT = \frac{C}{k_B[3 + \exp\left(\Delta E_{S-T}/k_B T\right)]}$$

Where I is the EPR intensity, C is a constant, k_B is Boltzman's constant, T is the temperature and $\Delta E_{s\text{-}t}$ is correlated to the excitation energy from the singlet ground state to the triplet excited state.

Single-crystal X-ray diffraction data of **Eu-TPTB** was collected using an Oxford Cryo stream system on a XtaLAB PRO MM007-DW diffractometer system equipped with a RAMicro7HF-MR-DW(Cu/Mo) X-ray generator and Pilatus3R-200K-A detector (Rigaku, Japan, Cu Kα, λ = 1.54178 Å) at 100 K but the **Yb-TPTB** was collected on Bruker AXS Apex II CCD diffractometer (Cu Kα, λ = 1.54178 Å) at 150 K. The numerical absorption corrections were applied using the program of ABSCOR. The space group was assigned and the structure was solved by direct methods using XPREP within the SHELXTL suite of programs[S1] and refined by full matrix least squares against F^2 with all reflections using Shelxl2018[S2] using the graphical interface Olex2[S3], which yielded the positions of all non-hydrogen atoms, and they were refined anisotropically. Hydrogen atoms were placed in calculated positions with fixed isotropic thermal parameters and included in the structure factor calculations in the final stage of full-matrix least-

squares refinement. All calculations were performed using the SHELXTL system of computer programs. The unit cell volume included a large region of disordered solvent which could not be modelled as discrete atomic sites. The treatment for the guest molecules in the cavities of all crystals involves the use of the SQUEEZE program of PLATON. Crystal data and structure refinement parameters are summarized in Table S1. Complete crystallographic data for **Eu-TPTB** and **Yb-TPTB**, in CIF format, have been deposited with the Cambridge Crystallographic Data Centre as CCDC number 2190182-2190183. These data can be obtained free of charge from The Cambridge Crystallographic Data Centre *via* www.ccdc.cam.ac.uk/data_request/cif.

Computational details

Density Functional Theory (DFT) calculation was used to study the nature of the biradical on contracted H_3TPTB linkers resulting from thermal annealing. Geometry optimizations and frequency calculation[S4] of singlet and triplet H_3**TPTB** were performed using ORCA 4.2.1[S5] with B3LYP[S6] functional for density-fitting approximation and def2-TZVP(-f)[S7, S8] basis set. The multiplicity of the structure was set to be triplet consistent with biradical state. In the geometry optimization, the default tight convergence in the SCF cycle was adopted without any orbital symmetry constraints. The optimized structure was confirmed to be energetically at its local minimum without imaginary/negative frequencies before further calculation. Mulliken population analysis spin natural orbital (SNO) by Hirshfeld method[S9] and spin density analysis were performed using Multiwfn 3.7 software package[S10]. Spin density, and SNOs were plotted with VMD 1.9.3[S11].

The time-dependent-DFT (TD-DFT) calculation is based on the orbit premise of RI-wB97X-D3/def2-SV(P) single-point calculation[S12]. The solid-state UV-Vis absorption spectra reported in this work were measured in the spectral region of 200–2500 nm. Singlet and triplet H_3**TPTB** were used as models for probing the effect by diradicals on the absorption profiles. The simulated absorption profiles were obtained using B3LYP functional of TD-DFT with PBE0 basis set. Fully optimized ground-state structures of singlet and triplet H_3**TPTB** based on TD-DFT/J RIJCOSX/def2-SV(P) calculations were used to compute the vertical excitation energies, oscillator strength and absorption wavelength of the simulated absorption profiles. As per the Frank–Condon principle, the maximum absorption peaks (λ_{max}) in absorption spectra correspond to vertical excitation[S13].

Evaluation of the solar evaporation.

All the solar water evaporation experiments were conducted under a 300 W Xenon lamp (PLS-SXE300, Perfect light, Beijing) with a 420 nm cut filter to simulate the solar irradiance. The light intensity at the sample surface is adjustable. The optical power on the surface was measured by a power meter (CEL-NP2000-2A, Beijing Aulight Co. Ltd., China). For solar evaporation, the solar absorber samples were placed on top of a quartz beaker (The inner diameter is 22 mm and the outer diameter is 25 mm) filled with pure water. To evaluate the water evaporation performance of the solar absorber, the weight loss of the cylindrical container was recorded in real time fashion using a computer controlled electronic balance (PTX-FA110S, HUAZHI, 0.1 mg) and the temperature over the process was recorded by an IR thermal camera (Thermo X, Shanghai Magnity Technologies Electronics Co. Ltd.). All experiments were performed under room temperature of 23 ± 1 °C and humidity of about 60%.

Calculation of the efficiency for solar to vapor generation

The conversion efficiency η of solar energy in photothermally assisted water evaporation was calculated as the following formula. [S14]

$$\eta = \frac{\dot{m}h_{LV}}{C_{opt}P_0}$$

Where $\dot{m}$ refers to the evaporation rate of water, h_{LV} refers to the total liquid vapor phase-change enthalpy (the sensible heat and the enthalpy of vaporization, and, $h_{LV} = Q + \Delta h_{vap}$), Q is the energy provided to heat the system from the initial temperature to a final temperature, Δh_{vap} is the latent heat of vaporization of water, P_0 is the nominal solar irradiation value of 0.1 W cm^{-2}, and C_{opt} represents the optical concentration. The schematic for the vaporization enthalpy of the vapor is displayed as follows:

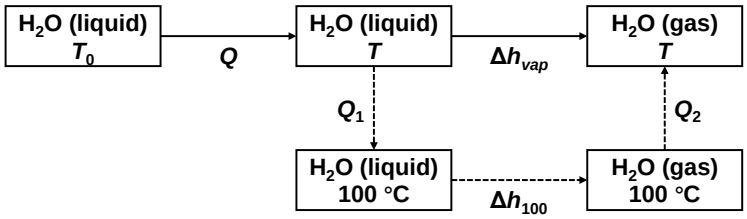

$$Q = C_{liquid} \times (T - T_0)$$

$$\Delta h_{vap} = Q_1 + \Delta h_{100} + Q_2$$

$$Q_1 = C_{liquid} \times (100 - T)$$

$$Q_2 = C_{vapor} \times (T - 100)$$

In this study, C_{liquid}, the specific heat capacity of liquid water is a constant of 4.18 J g^{-1} °C^{-1}. C_{vapor}, the specific heat capacity of water vapor is a constant of 1.865 J g^{-1} °C^{-1}. Δh_{100} is the latent heat of vaporization of water at 100 °C, taken to be 2260 J g^{-1}.

Experimental procedures

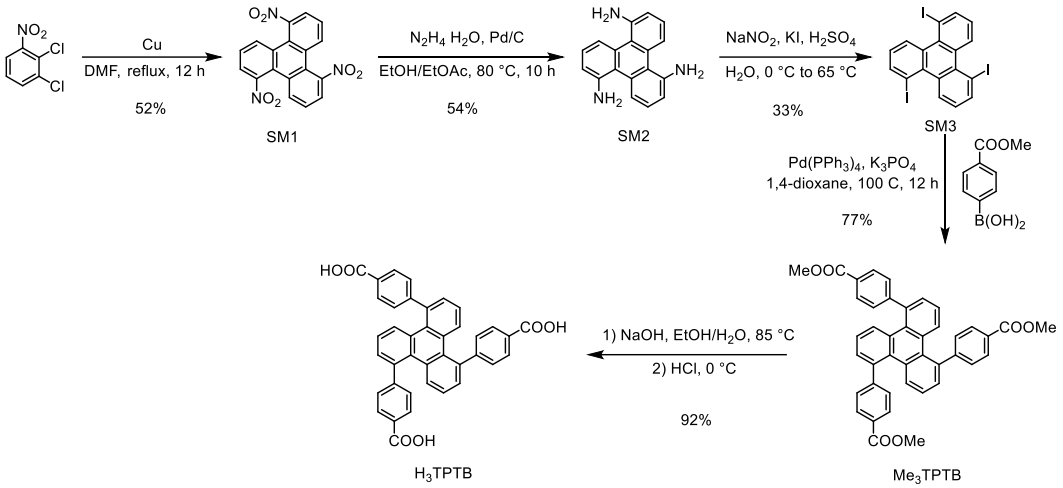

Scheme S1. The synthetic scheme for H_3**TPTB**

Synthesis of 1,5,9-Trinitrotriphenylene (**SM1**)

SM1 was synthesized according to the previously reported procedure.[S15] To a solution of 2,3-dichloronitrobenzene (30.0 g, 156.3 mmol) in DMF (240 mL) was added copper powder (60.0 g, 937.5 mmol). The mixture was stirred at reflux for 12 hours under N_2 atmosphere. After cooling to 120 ℃, the hot solution was filtered through diatomite and washed by DMF (3 × 40 mL) to remove the excess copper powder. The filtrate was then slowly poured into a diluted ammonia solution 1.2 L (containing 300 mL conc. $NH_3 \cdot H_2O$) with vigorous stirring. A black solid precipitated and the aqueous layer was decanted. The solid was crushed into small pieces and washed with diluted ammonia solution and water successively. The desired product **SM1** was obtained as a yellow solid after purification by column chromatography packed with silica gel using petroleum ether/dichloromethane (3:2, v/v) as eluent. Yield: 9.83 g (52%, based on 2,3-dichloronitrobenzene). ^{1}H NMR (400 MHz, $CDCl_3$) δ (ppm) 8.15 (d, J = 8.2 Hz, 3H), 7.93 (d, J = 7.6 Hz, 3H), 7.68 (dd, J = 8.0 Hz, 3H); ^{13}C NMR (100 MHz, $CDCl_3$) δ (ppm) 149.58, 129.52, 128.33, 128.25, 125.37, 122.39.

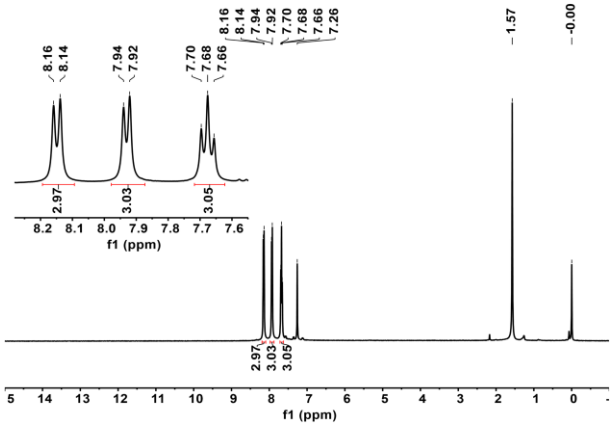

The ^{1}H NMR spectrum of compound **SM1** in $CDCl_3$

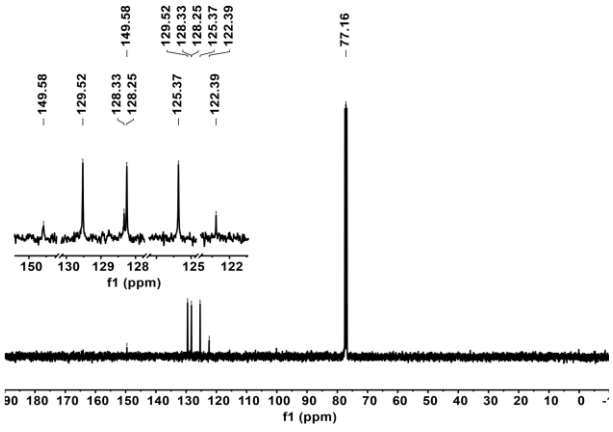

The ^{13}C NMR spectrum of compound **SM1** in $CDCl_3$

Synthesis of triphenylene-1,5,9-triamine (**SM2**)

SM2 was synthesized according to the previously reported procedure.[S15] Activated palladium on carbon (10% w/w, 0.60 g) was added to a solution of **SM1** (2.0 g, 5.5 mmol) in ethyl acetate (30 mL) and EtOH (25 mL) under N_2 atmosphere, and the mixture was heated at 80 °C. Then $N_2H_4 \cdot H_2O$ (80%, 10 mL) was added dropwisely to the hot solution. After refluxing for 10 hours, the solution was taken off by filtration and the solids were washed with ethyl acetate. The filtrate was concentrated under reduced pressure and purified by column chromatography packed with silica gel using petroleum ether/ethyl acetate (5:1, v/v) as eluent to give **SM2** as a yellow solid. Yield: 812 mg (54%, based on **SM1**). ^{1}H NMR (400 MHz, DMSO-d_6) δ (ppm) 8.21 (d, J = 8.1 Hz, 3H), 7.16 (dd, J = 7.9 Hz, 3H), 6.87 (d, J = 7.8 Hz, 3H), 5.33 (s, 6H); ^{13}C NMR (100 MHz, DMSO-d_6) δ (ppm) 145.68, 131.90, 126.11, 117.78, 114.50, 113.51.

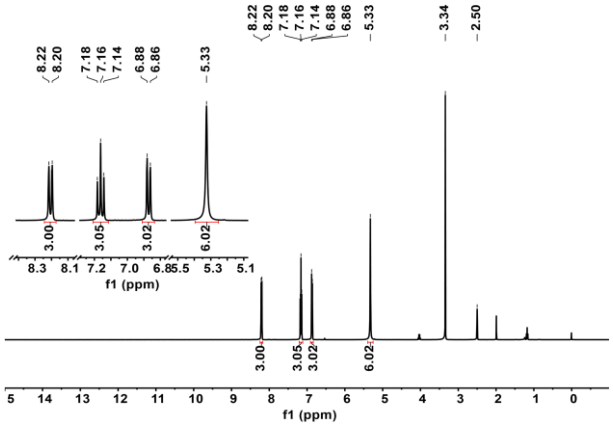

The ^{1}H NMR spectrum of compound **SM2** in DMSO-d_6

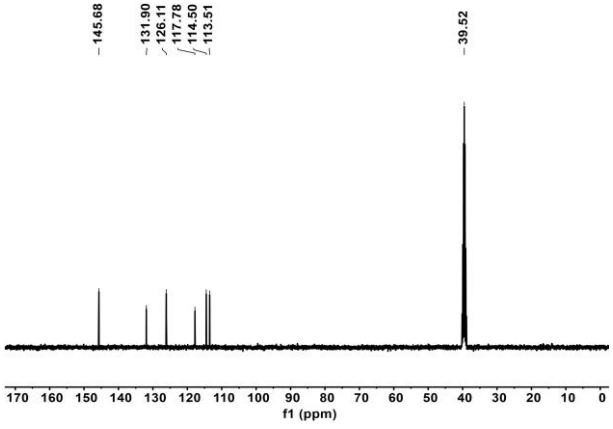

The ^{13}C NMR spectrum of compound **SM2** in DMSO-d_6

Synthesis of 1,5,9-Triiodotriphenylene (**SM3**)

SM3 was synthesized according to the previously reported procedure.[S16] A suspension of the triaminotriphenylene **SM2** (4.0 g, 14.6 mmol) in a solution of sulfuric acid (30.0 mL) and water (45 mL) was cooled to 0 ℃ by an ice bath. A solution of sodium nitrite (4.0 g, 58.5 mmol) in water (40 mL) was added dropwisely with stirring. The resulting brown solution was poured into a vigorously stirred solution of potassium iodide (38.9 g, 234 mmol) in water (60 mL) in a 2.0 L single-neck conical flask, during which foam was generated. After stirring for one hour at room temperature, the reaction was heated at 65 ℃ by a water bath until the foaming disappeared. The solid was filtered, washed with water and dilute sodium thiosulfate solution, successively. The solid was extracted with dichloromethane (1 × 500 mL, 2 × 50 mL), and the insoluble solid was filtered off. The combined organic fraction was washed with sodium thiosulfate solution, dried with anhydrous sodium sulfate and filtered. After removal of the solvent in vacuum and purification by column chromatography packed with silica gel using petroleum ether as eluent, compound **SM3** was obtained as a white solid (2.9 g, 33% yield based on **SM2**). ^{1}H NMR (400 MHz, $CDCl_3$) δ (ppm) 9.19 (d, J = 8.1 Hz, 3H), 8.23 (d, J = 7.6 Hz, 3H), 7.15 (dd, J = 7.9 Hz, 3H); ^{13}C NMR (100 MHz, $CDCl_3$) δ (ppm) 143.12, 133.00, 132.72, 127.58, 126.32, 90.83.

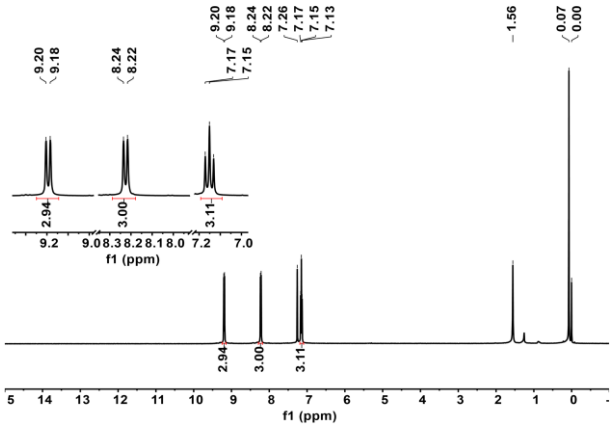

The ^{1}H NMR spectrum of compound **SM3** in $CDCl_3$

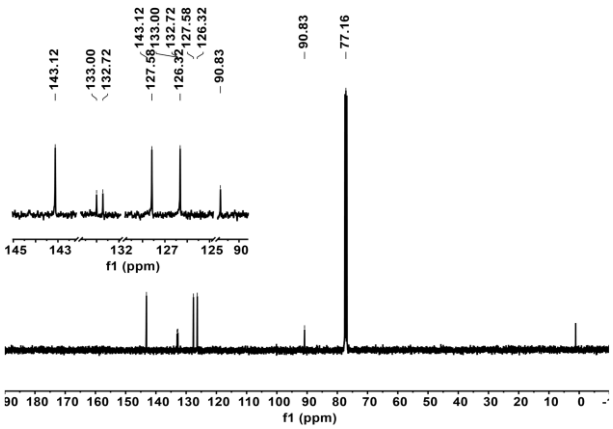

The ^{13}C NMR spectrum of compound **SM3** in $CDCl_3$

Synthesis of trimethyl 4,4',4''-(triphenylene-1,5,9-triyl)tribenzoate (**SM4**)

A Schlenk tube was charged with a magnetic stirring bar, 1,5,9-triiodotriphenylene (606 mg, 1.0 mmol), tetrakis(triphenylphosphine)palladium (57 mg, 0.05 mmol), (4-(methoxycarbonyl)phenyl)boronic acid (1.08 g, 6 mmol) and anhydrous potassium carbonate (552 mg, 4.0 mmol). The Schlenk tube was then connected to a vacuum gas manifold and the suspension inside was bubbled with N_2 gas for five minutes. 1,4-dioxane (20 mL, bubbled with N_2 gas for five minutes) was injected into the mixture *via* cannula under a positive N_2 pressure. The Schlenk tube was then stoppered and stirred at 100 °C for 24 hours. After cooling to room temperature, the reaction mixture was poured into 100 mL of a petroleum ether/ethyl acetate mixture (1:1, v/v), filtered through a silica gel plug and rinsed with a petroleum ether/ethyl acetate mixture (1:1, v/v). The solvents were then removed on a rotary evaporator and the brown residue was purified by silica gel column chromatography using petroleum ether/ethyl acetate (5:1, v/v) to provide a light-yellow solid product (452.4 mg, 77% yield based on **SM3**). ^{1}H NMR (400 MHz, $CDCL_3$) δ (ppm) 8.10 (d, J = 8.3 Hz, 6H), 7.57 (d, J = 7.3 Hz, 3H), 7.46 (d, J = 8.3 Hz, 6H), 7.31 (d, J = 6.3 Hz, 3H), 7.06 (dd, 3H), 3.97 (s, 9H); ^{13}C NMR (100 MHz, $CDCl_3$) δ (ppm) 167.18, 149.88, 139.03, 131.23, 131.02, 130.39, 129.96, 129.46, 129.35, 128.77, 124.93, 52.31.

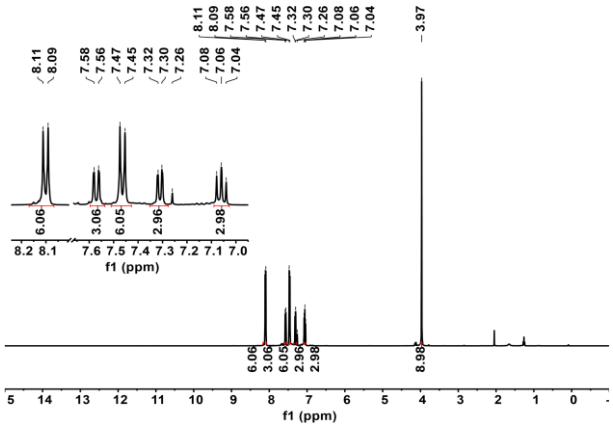

The ^{1}H NMR spectrum of compound **SM4** in $CDCl_3$

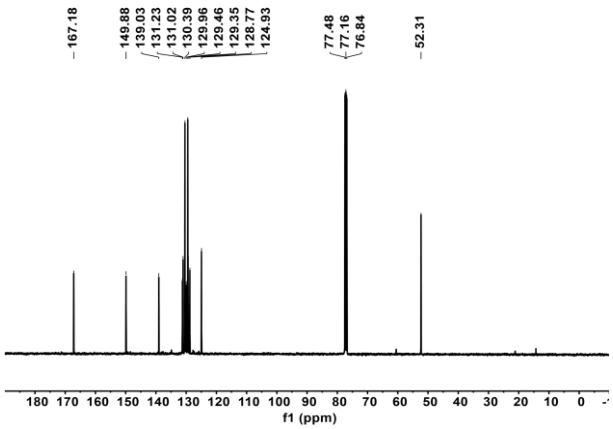

The ^{13}C NMR spectrum of compound **SM4** in $CDCl_3$

Synthesis of 4,4',4''-(triphenylene-1,5,9-triyl)tribenzoic acid (H_3**TPTB**)

A suspension of the **SM4** (1.2 g, 1.9 mmol) and NaOH (1.6 g, 40 mmol) in EtOH/H_2O (20 mL, 1:1 v/v, bubbled with N_2 gas for 5 minutes) was injected into the mixture *via* cannula under a positive N_2 pressure. After being stirred at 85 ℃ for 12 hours, the mixture was poured into water (100 mL) and HCl (10%) was then added slowly with vigorous stirring. After the pH value of the mixture became lower than 4, the precipitate was collected by suction filtration and washed with water extensively to provide white solid product (233 mg，85% yield based on **SM4**). ^{1}H NMR (400 MHz, DMSO-d_6) δ (ppm) 13.04 (s, 3H), 8.02 (d, J = 8.2 Hz, 6H), 7.51 (d, J = 8.4 Hz, 3H), 7.48 (d, J = 8.2 Hz, 6H), 7.36 (d, J = 6.9 Hz, 3H), 7.16 (dd, J = 7.8 Hz, 3H); ^{13}C NMR (100 MHz, DMSO-d_6) δ (ppm) 167.76, 149.38, 139.32, 131.62, 131.09, 130.78, 129.82, 129.73, 129.14, 125.63, 39.52.

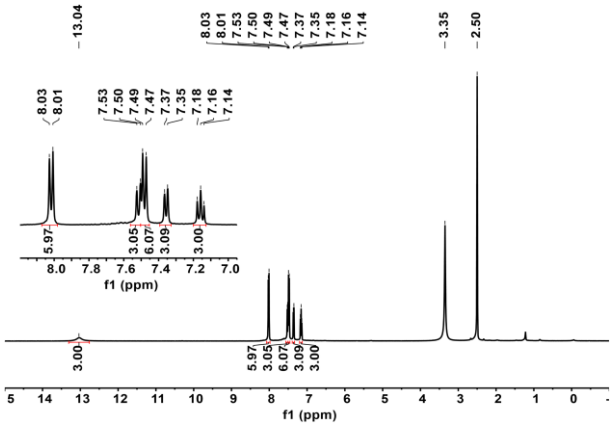

The ^{1}H NMR spectrum of compound H_3**TPTB** in DMSO-d_6

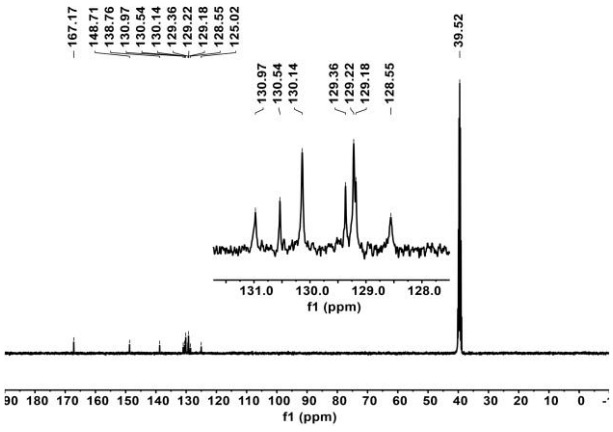

The ^{13}C NMR spectrum of compound H_3**TPTB** in DMSO-d_6

Preparation of single crystals of **Eu-TPTB** and **Yb-TPTB**.

H_3**TPTB** (10.0 mg, 17.0 μmol) and $EuCl_3 \cdot 6H_2O$ (15.0 mg, 33.4 μmol) were loaded into a heavy-wall glass tube (10 mm OD, 6 mm ID), and then a solution of *N,N*-dimethylformamide and water (1.3 mL, 10:3, v/v) was added. The tube was then flame-sealed and heated at 90 °C in a programmable oven for 24 hours followed by cooling (1 °C/minute) to room temperature. The resultant single crystals were then retrieved by filtration, washed with DMF and acetone for three times to give colorless **Eu-TPTB** crystal suitable for single-crystal X-ray diffraction (9.5 mg, yield 75.8% based on H_3**TPTB**). The **Yb-TPTB** crystal could be obtained by using $YbCl_3 \cdot 6H_2O$ in place of $EuCl_3 \cdot 6H_2O$ under the same conditions (10.5 mg, yield 81.5% based on H_3**TPTB**).

Preparation of powder of **Eu-TPTB** and **Yb-TPTB**.

H_3**TPTB** (100.0 mg, 170.0 μmol) was dissolved in 10 mL DMF and heated at 90 °C for 30 minutes. Afterwards, $YbCl_3 \cdot 6H_2O$ (150.0 mg, 334.0 μmol) dissolved in 3 mL H_2O was added to the above solution with stirring. The mixture was heated at 90 °C for five hours followed by cooling to room temperature. The resultant white suspension was then filtered. The white solid was washed with DMF and acetone to give white powder. **Eu-TPTB** was activated by Soxhlet extraction in acetone solution for two days before vacuum drying at 60 °C for five hours (102.7 mg, yield 82.0% based on H_3**TPTB**). The **Yb-TPTB** could be obtained by using $YbCl_3 \cdot 6H_2O$ in place of $EuCl_3 \cdot 6H_2O$ under the same conditions. (115.2 mg, yield 89.4% based on H_3**TPTB**)

Preparation of thermally annealed **Eu-TPTB@PU** and **Yb-TPTB@PU**.

Since thermally annealed **Eu-TPTB**/**Yb-TPTB** has a strong graininess, it easily falls off PU foam in aqueous solution. Therefore, polycaprolactone (PCL) was introduced as a binder to bind thermally annealed **Eu-TPTB**/**Yb-TPTB** to PU foam. The specific operation is as follows: 20 mg thermally annealed **Eu-TPTB**/**Yb-TPTB** was dispersed in 1 mL PCL solution (5 mg/mL, in dichloromethane), ultrasonicated for 10 minutes, and added in dropwise fashion evenly on the PU foam. The composite was then placed in an oven at 40 °C for five hours.

Supporting Figures

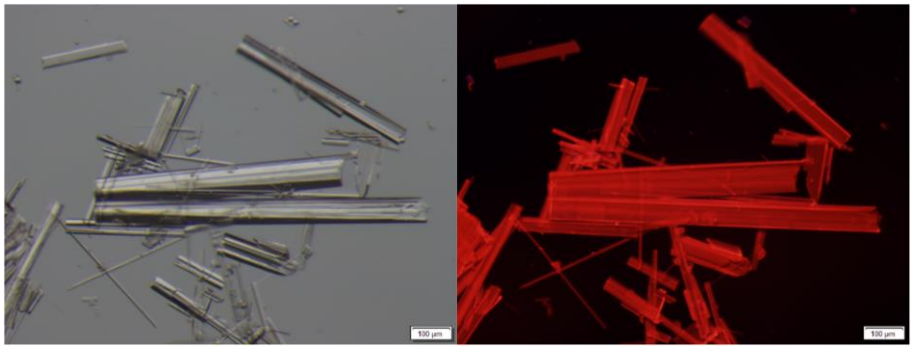

Fig. S1. The photographs of **Eu-TPTB** crystal in natural light (left), and under 365 nm UV light (right); scale bar: 100 μm.

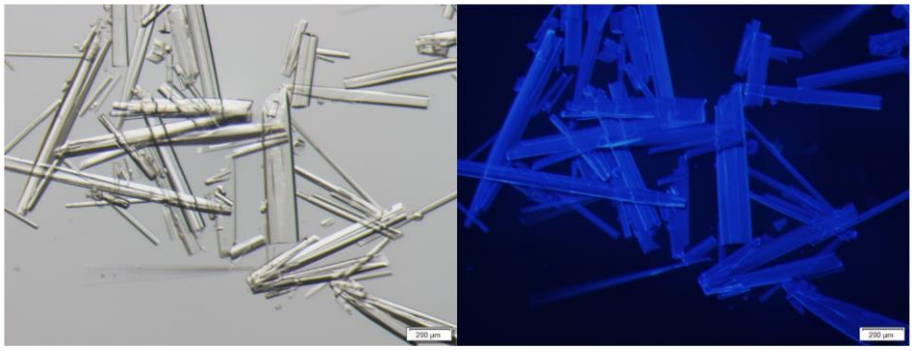

Fig. S2. The photographs of **Yb-TPTB** crystal in natural light (left), and under 365 nm UV light (right); scale bar: 200 μm.

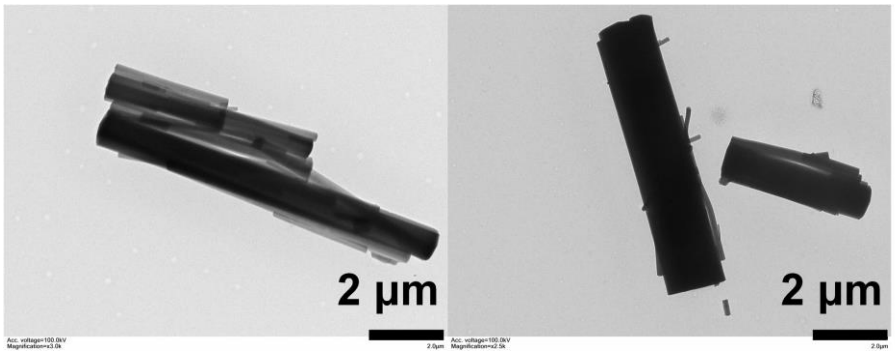

Fig. S3. The TEM images of **Eu-TPTB** (left) and **Yb-TPTB** (right); scale bar: 2.5 μm.

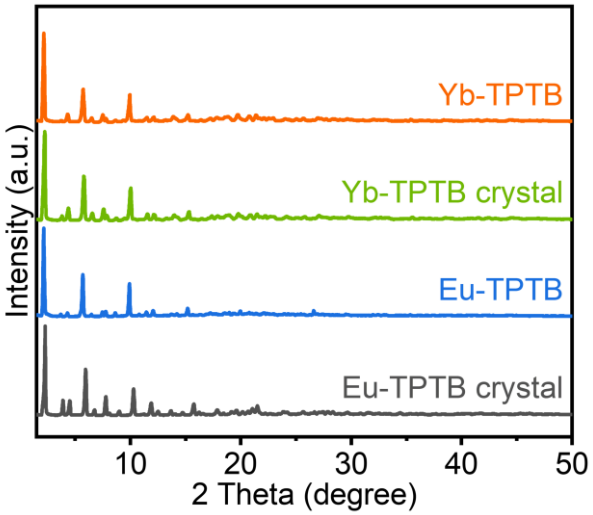

Fig. S4. The PXRD patterns of **Eu-TPTB crystal**, **Eu-TPTB**, **Yb-TPTB crystal**, **Yb-TPTB**.

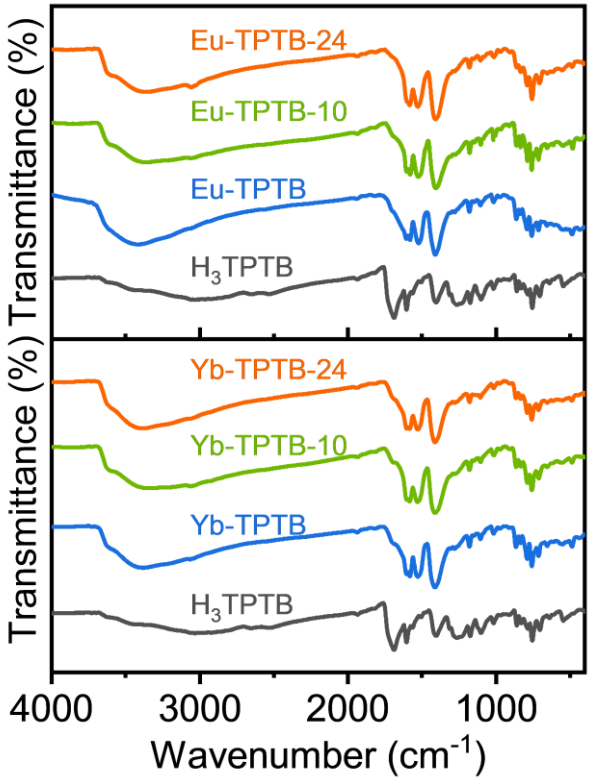

Fig. S5. The FT-IR spectra of pristine or thermally annealed **Eu-TPTB** and **Yb-TPTB**.

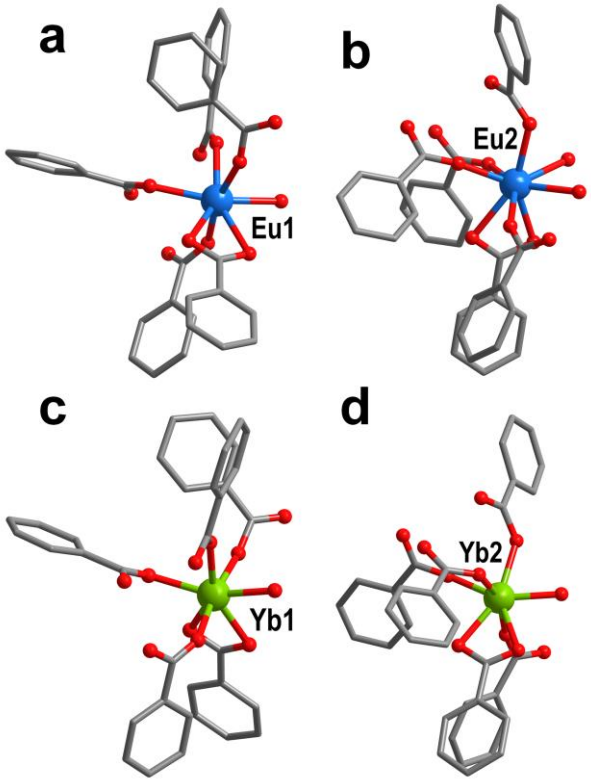

Fig. S6. The coordination environments of Eu^{3+} and Yb^{3+} centers in **Eu-TPTB** and **Yb-TPTB**, respectively.

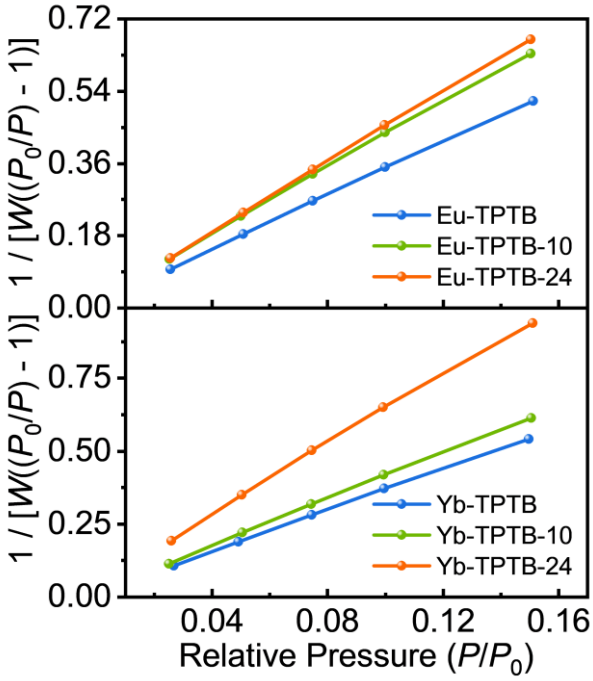

Fig. S7. The BET plots of pristine or thermally annealed **Eu-TPTB** (top) and **Yb-TPTB** (down).

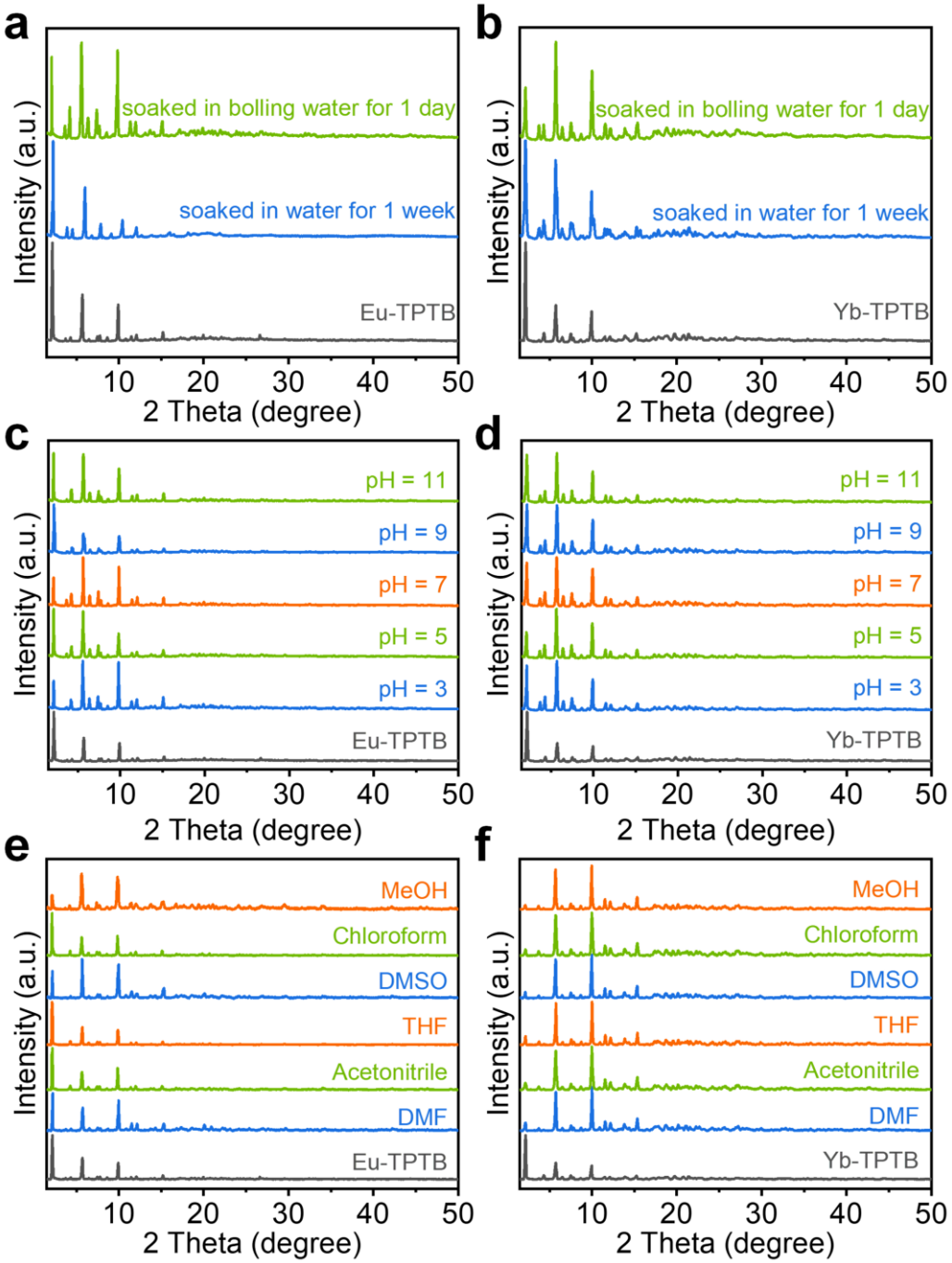

Fig. S8. The stability test of **Eu-TPTB** and **Yb-TPTB**. The PXRD patterns of **Eu-TPTB** (a) and **Yb-TPTB** (b) soaked in water for one week or boiling water for one day; the PXRD patterns of **Eu-TPTB** (c) and **Yb-TPTB** (d) soaked in different pH solutions for one day; the PXRD patterns of **Eu-TPTB** (e) and **Yb-TPTB** (f) soaked in common organic solvents for one day.

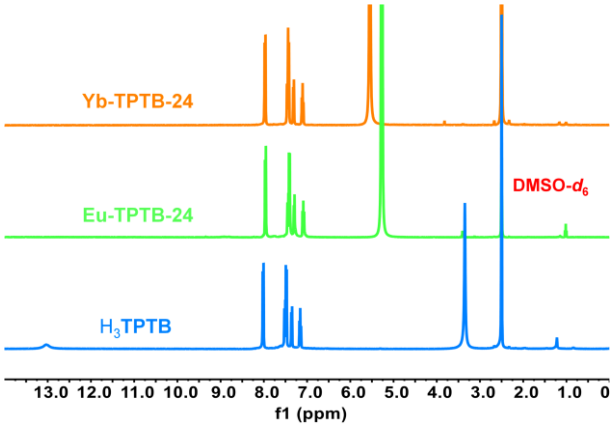

Fig. S9. The ^{1}H NMR spectra of the linker decomposed from **Yb-TPTB-24** (orange), **Eu-TPTB-24** (green) and the pristine ligand, H_3**TPTB** (blue).

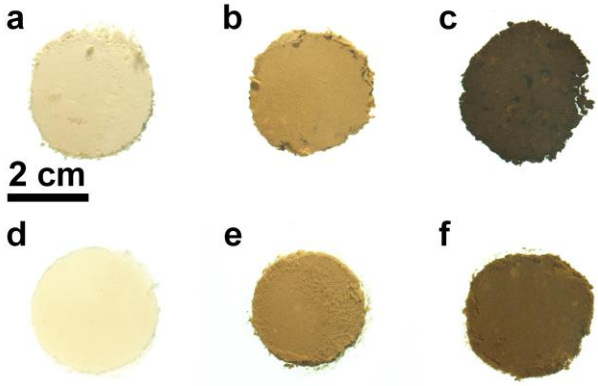

Fig. S10. The photographs of pristine and thermally annealed **Eu-TPTB** and **Yb-TPTB** powder, (a) **Eu-TPTB**, (b) **Eu-TPTB-10**, (c) **Eu-TPTB-24**, (d) **Yb-TPTB**, (e) **Yb-TPTB-10**, (f) **Yb-TPTB-24**.

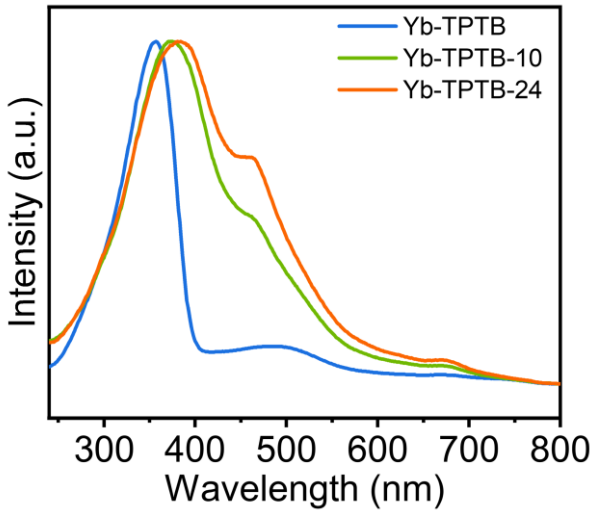

Fig. S11. The excitation spectra of **Yb-TPTB**, **Yb-TPTB-10**, and **Yb-TPTB-24** (λ_{em} = 980 nm).

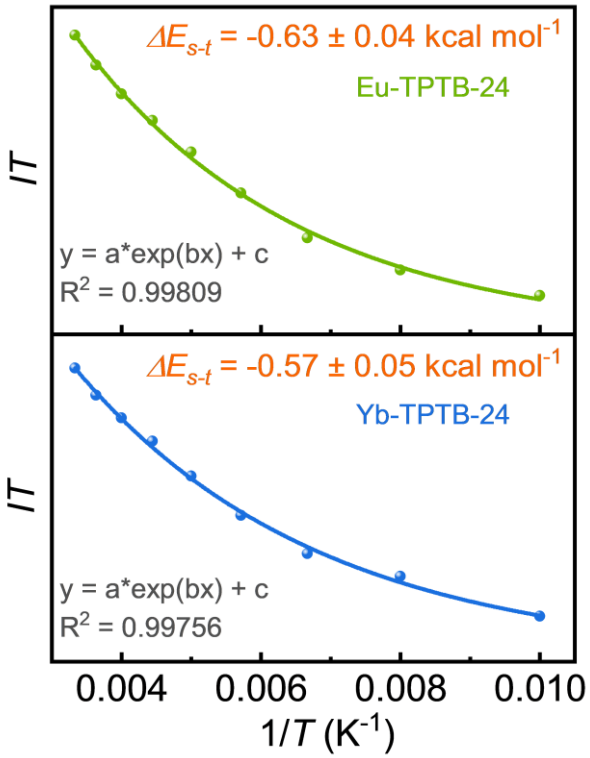

Fig. S12. The $IT-1/T$ curves based on the VT-EPR data of **Eu-TPTB-24** (top) and **Yb-TPTB-24** (down) in solid state; I: EPR intensity; T: temperature (in K).

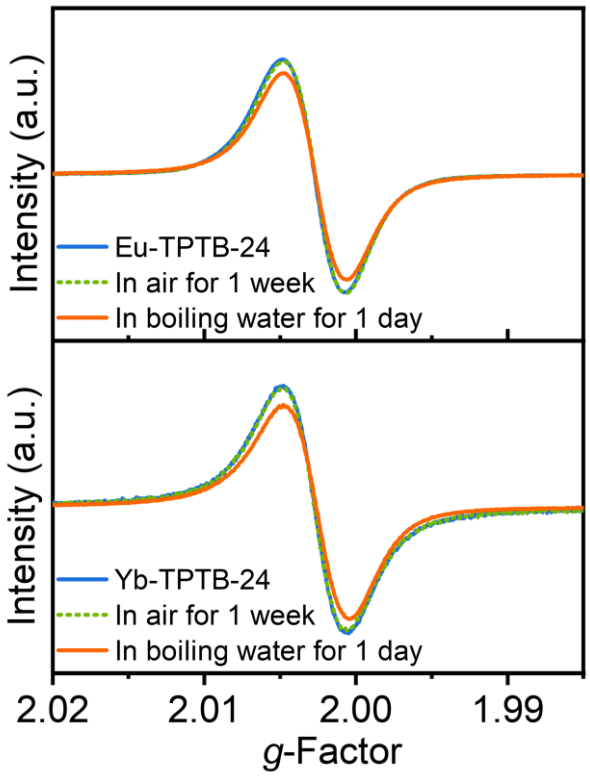

Fig. S13. The EPR spectra of **Eu-TPTB-24** (top) and **Yb-TPTB-24** (down) placed in air and boiling water.

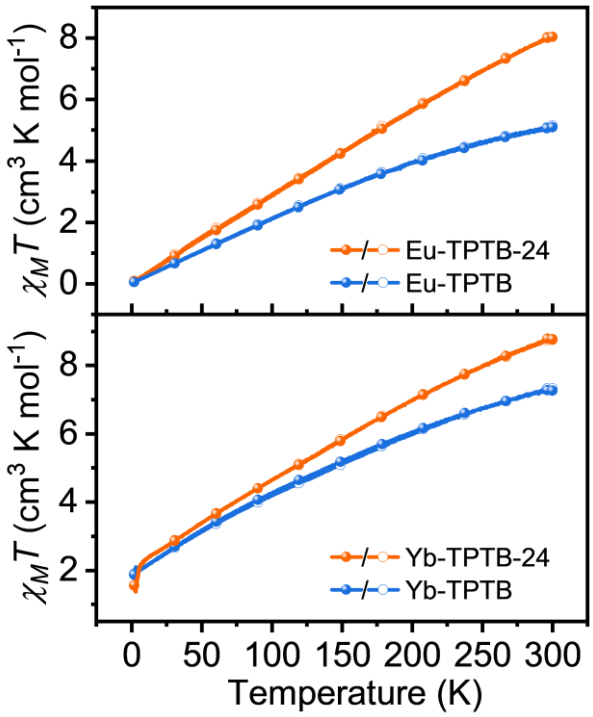

Fig. S14. The plots of $\chi_M T$ versus T for **Eu-TPTB**, **Yb-TPTB**, **Yb-TPTB-24** and **Eu-TPTB-24** at 1000 Oe

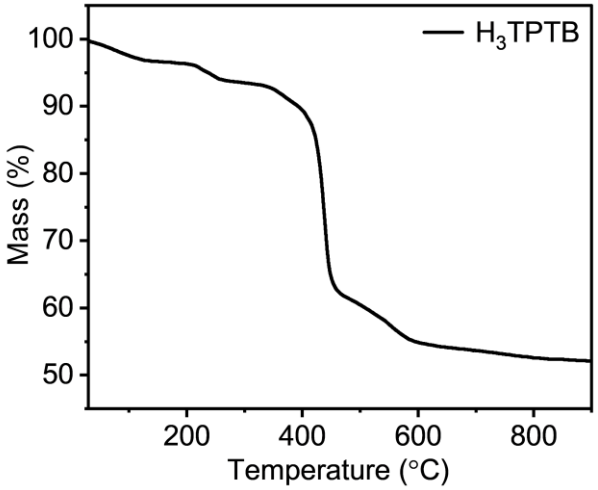

Fig. S15 The TGA curve of H_3**TPTB** in the N_2 atmosphere, heating rate with 5 °C/min.

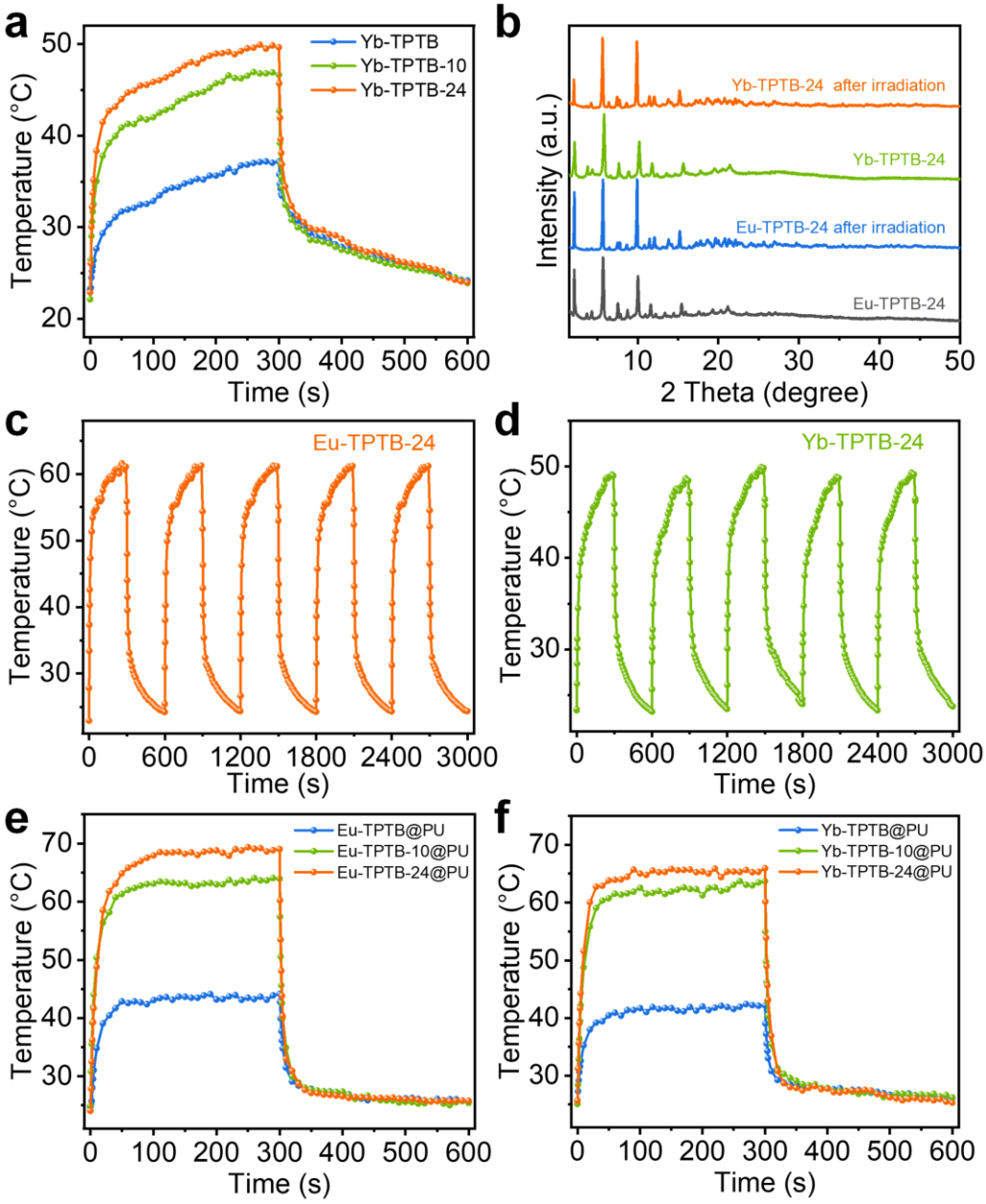

Fig. S16 The photothermal conversion behaviour of pristine and annealed **Eu-TPTB** and **Yb-TPTB**. (a) Temperature variation of **Yb-TPTB**, **Yb-TPTB-10** and **Yb-TPTB-24** under Xenon lamp (0.1 W cm^{-2}) irradiation; (b) the PXRD patterns of **Eu-TPTB-24** and **Yb-TPTB-24** before and after irradiation by Xenon lamp; anti-photobleaching property of **Eu-TPTB-24** (c) and **Yb-TPTB-24** (d) in five illumination cycles; temperature variation of pristine and thermally annealed **Eu-TPTB** (e) and **Yb-TPTB** (f) loaded on PU foams under Xenon lamp (0.1 W cm^{-2}) irradiation

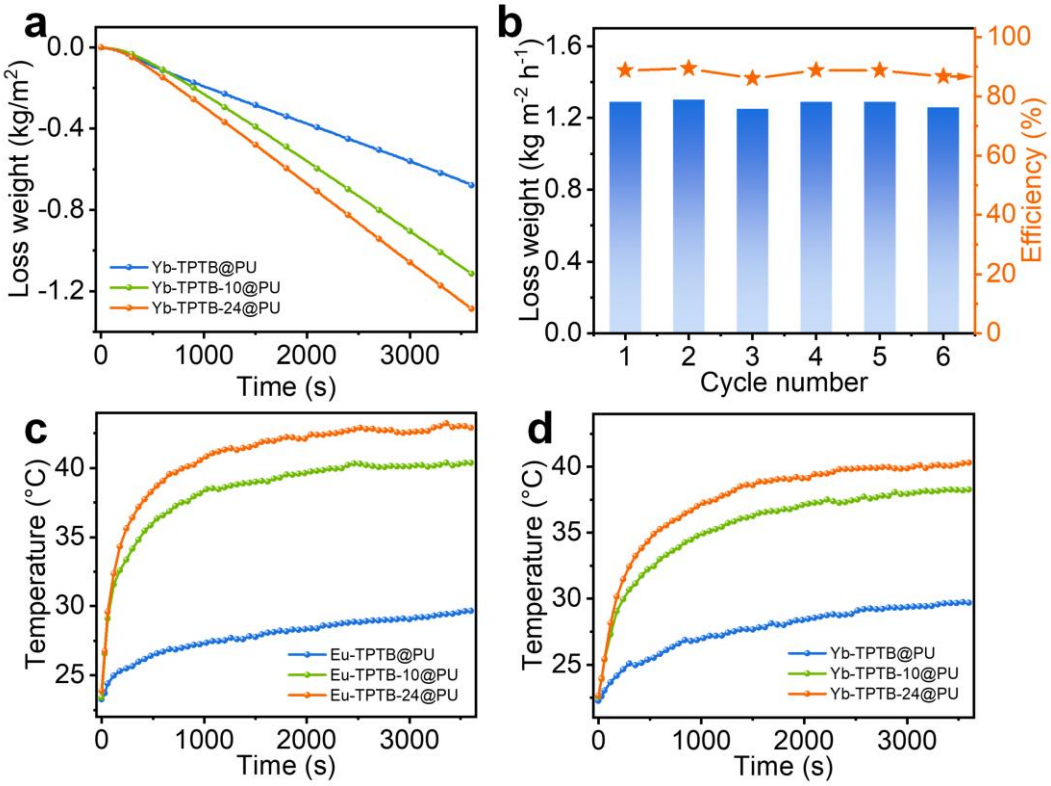

Fig. S17. Water evaporation of pristine or thermally annealed **Eu-TPTB** and **Yb-TPTB** loaded on PU foam. (a) water evaporation rate of pristine or thermally annealed **Yb-TPTB** loaded on PU foam under Xenon lamp (0.1 W cm^{-2}) irradiation; (b) the solar-energy to vapour evaporation rate and efficiency of **Yb-TPTB-24** loaded on PU foams in six cycles; the surface temperatures of pristine or thermally annealed **Eu-TPTB** (c) and **Yb-TPTB** (d) loaded on PU foam during water evaporation.

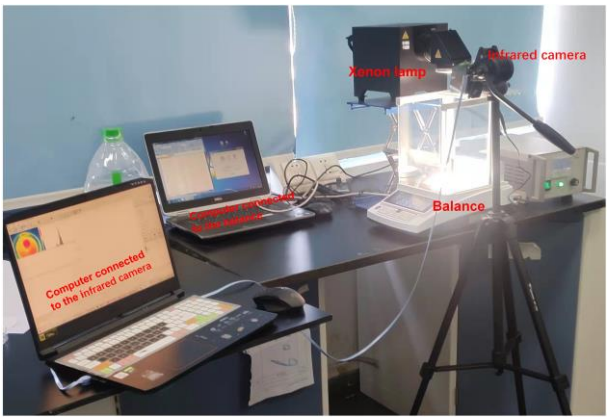

Fig. S18. The schematic diagram of solar-driven water evaporation device.

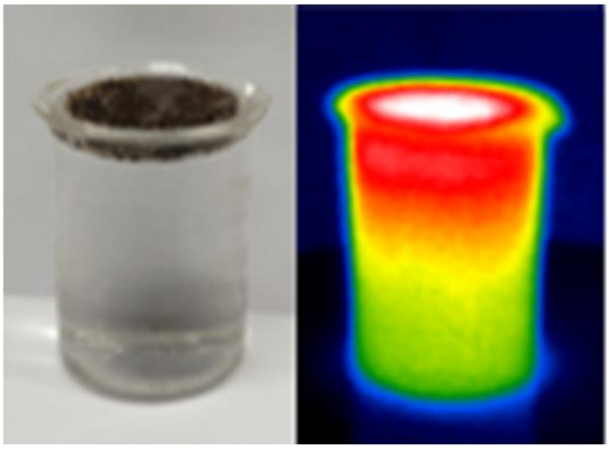

Fig. S19. The natural light photo (left) and infrared thermal images (right) of **Eu-TPTB-24@PU** during water evaporation illustrating that the energy conversion occurs at the PU foams.

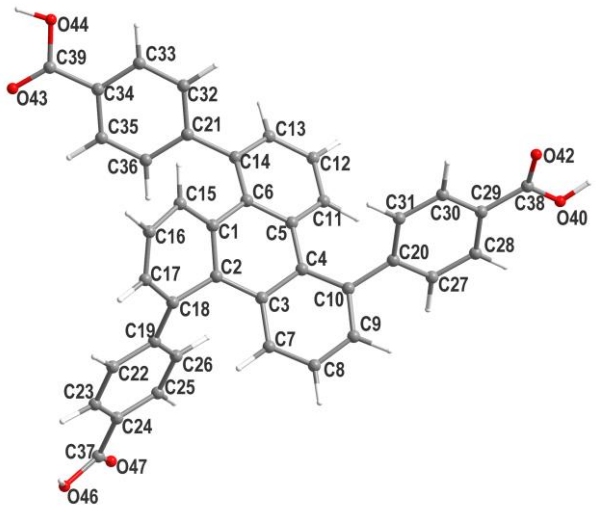

Fig. S20. Atom labels of H_3**TPTB** (hydrogen labels are omitted for clarity).

Supplementary Tables

Table S1. Crystal data and structure refinement for **Eu-TPTB** and **Yb-TPTB**.

Compound	Eu-TPTB	Yb-TPTB
Empirical formula	$C_{78}H_{48}Eu_2O_{15}$	$C_{78}H_{46}O_{14}Yb_2$
Formula weight	1529.08	1553.23
Temperature (K)	100	150
Crystal system	trigonal	trigonal
Space group	*R-3*	*R-3*
a (Å)	79.5824(12)	80.680(5)
b (Å)	79.5824(12)	80.680(5)
c (Å)	10.3300(3)	10.1783(10)
α (deg)	90	90
β (deg)	90	90
γ (deg)	120	120
Volume (Å^3)	56658(2)	57376(9)
Z	18	18
D_c (g cm^{-3})	0.807	0.809
F(000)	13716	13788
Reflections collected	49484	35772
GOF	1.031	1.028
Final R indexes [I>=2σ (I)]	R_1[a]= 0.0910, wR_2[b] = 0.2751	R_1[a]= 0.1210, wR_2[b] = 0.3009
Final R indexes [all data]	R_1[a]= 0.1141, wR_2[b] = 0.2941	R_1[a]= 0.1397, wR_2[b] = 0.3128

[a] $R_1 = \sum||Fo| - |Fc|| / \sum(|Fo|)$, [b] $wR_2 = \{\sum[w(Fo^2 - Fc^2)^2] / \sum[w(Fo^2)^2]\}^{1/2}$

Table S2. The selected Ln–O bonds length calculated from single crystal structure[a].

Number	Atom1	Atom2	Length (Å)	Atom1	Atom2	Length(Å)
1	Eu1	O1	2.293(8)	Yb1	O1	2.20(1)
2	Eu1	O3	2.469(8)	Yb1	O5	2.30(1)
3	Eu1	O4	2.47(1)	Yb1	O8	2.305(7)
4	Eu1	O6	2.317(5)	Yb1	O9	2.383(9)
5	Eu1	O7	2.265(8)	Yb1	O10	2.312(9)
6	Eu1	O11	2.381(8)	Yb1	O11	2.177(9)
7	Eu2	O2	2.328(7)	Yb2	O2	2.32(2)
8	Eu2	O5	2.414(8)	Yb2	O3	2.35(1)
9	Eu2	O8	2.378(7)	Yb2	O4	2.35(1)
10	Eu2	O9	2.430(5)	Yb2	O6	2.182(7)
11	Eu2	O10	2.486(6)	Yb2	O7	2.257(8)
12	Eu2	O12	2.273(7)	Yb2	O12	2.260(7)
Average			2.380	Average		2.283

[a]The Eu-O or Yb-O bonds of coordinated water were omitted for clarity.

Table S3. Water evaporation rates and solar-vapor efficiencies of the pristine and thermally annealed **Eu-TPTB** and **Yb-TPTB**.

	T_0 (°C)	T (°C)	ΔT (°C)	$\dot{m}$ (kg m^{-2} h^{-1})	η (%)
Eu-TPTB	23.26	29.67	6.41	0.67	45.59
Eu-TPTB-10	23.39	40.37	16.98	1.26	86.42
Eu-TPTB-24	**23.87**	**42.90**	**19.03**	**1.45**	**99.56**
Yb-TPTB	22.27	29.70	7.43	0.68	46.35
Yb-TPTB-10	22.59	38.24	15.65	1.11	76.11
Yb-TPTB-24	22.67	40.31	18.64	1.29	88.73

Table S4. Cartesian coordinates for singlet H_3**TPTB**.

Atomic space	x	y	z
1(C)	66.66453633022033	-28.92915182555467	0.89558847923849
2(C)	66.63847091466413	-30.33565033828568	0.76258304600015
3(C)	67.90740813470957	-31.01440114314380	0.46372583995205
4(C)	69.07185274431352	-30.23695899278144	0.21172740085041
5(C)	68.89649101780992	-28.83016771344986	-0.15940274680459
6(C)	67.68134059544019	-28.18385886103149	0.16095296856250
7(C)	68.04563154748389	-32.40337233701889	0.62011667243580
8(C)	69.27652888784941	-33.01680217127551	0.54318467999338

9(C)	70.42343612007181	-32.24549374921273	0.39674190318533
10(C)	70.34370828373741	-30.86400999539160	0.27261692122820
11(C)	69.84993486349595	-28.13856418292239	-0.92226456083762
12(C)	69.64413792861525	-26.83316155540118	-1.31057826962314
13(C)	68.43343424714716	-26.20993823121652	-1.02870748211690
14(C)	67.42847059697604	-26.88317784938911	-0.34643256466687
15(C)	65.69671957454497	-28.28895663106211	1.68309335937941
16(C)	64.63115040273249	-28.99221783790031	2.19782210018245
17(C)	64.46093359415863	-30.32527733861885	1.83248010969224
18(C)	65.42187542683584	-31.00116896517138	1.09135920622540
19(C)	65.02643984132162	-32.31561199566445	0.53286618072943
20(C)	71.62739349187567	-30.11791537317181	0.32236923197224
21(C)	66.07546580196038	-26.26973713311898	-0.38841187644435
22(C)	64.41834661536279	-33.30236339666920	1.31150243581191
23(C)	63.94069853468977	-34.46816905516991	0.72940285332101
24(C)	64.03698438038413	-34.66722395054268	-0.64775112682007
25(C)	64.62986726684888	-33.67582571709089	-1.43228196450877
26(C)	65.12924829097661	-32.52807231849034	-0.84801514830091
27(C)	72.67352407438879	-30.43767203186919	-0.54682517804300
28(C)	73.88086951850920	-29.75812354295085	-0.48599577254396
29(C)	74.06870142637815	-28.75085196747467	0.46002171074636
30(C)	73.03699650478295	-28.44433227322513	1.35155681339671
31(C)	71.83170770148028	-29.11653559209876	1.27898430227283
32(C)	65.84232475667558	-24.97263459866453	0.07046595094718
33(C)	64.59219325288379	-24.38484838630457	-0.06473762082059
34(C)	63.55387603826752	-25.08248392275928	-0.68078889077511
35(C)	63.78331633010965	-26.37700704912223	-1.15261238494218
36(C)	65.02486403407066	-26.96120082271013	-1.00384561797156
37(C)	63.49143449864906	-35.87435129139478	-1.33817242881255
38(C)	75.33317796469028	-27.98493806358592	0.56316932609469
39(C)	62.20428223972015	-24.50404831703899	-0.87270736518437
40(O)	76.24600844208447	-28.32498683239857	-0.38379641383372
41(H)	77.02202197999874	-27.76613517444344	-0.22210712012827
42(O)	75.55925490314998	-27.13474856707636	1.39144545873540
43(O)	61.28311016057351	-25.06483764716171	-1.41778136627974
44(O)	62.08075020874741	-23.24809261736255	-0.37186005091360
45(H)	61.17053014773326	-22.97238321991175	-0.56125121395483
46(O)	63.37111412729355	-37.00295277218158	-0.58713829056559
47(O)	63.16217394139040	-35.88628136661807	-2.49330659716381
48(H)	63.79631112559807	-36.87898103786927	0.27158085027830
49(H)	67.18278432446532	-33.00750657080669	0.83915067493329
50(H)	69.35486397838866	-34.08927550194035	0.66667982403044
51(H)	71.39855886762895	-32.71309551537718	0.44130033762939

52(H)	70.75027896730869	-28.63603905896010	-1.23800983774917
53(H)	70.39841963810846	-26.31740634804975	-1.89015343375137
54(H)	68.22896761712047	-25.22407052957618	-1.42486914970588
55(H)	65.78788531184658	-27.23211771905179	1.88000617210866
56(H)	63.89452234472561	-28.49708065140895	2.81604328609271
57(H)	63.54470573587525	-30.83904261382691	2.09187021778675
58(H)	64.31726858393515	-33.15667810280303	2.37897376547111
59(H)	63.44971286732832	-35.19833183463265	1.36244695066403
60(H)	64.67700674192176	-33.82137659329732	-2.50275085924052
61(H)	65.58536940733123	-31.76428571729800	-1.46383292533784
62(H)	72.52739206578539	-31.20810588921652	-1.29256098116896
63(H)	74.67806233292443	-30.00467215812195	-1.17263035604117
64(H)	73.19911273151588	-27.67013539729979	2.08863792120514
65(H)	71.03006404990201	-28.86007276200667	1.95842867124039
66(H)	66.64601940784685	-24.42487872525897	0.54553221358486
67(H)	64.41931758407054	-23.38431932082262	0.30458563930904
68(H)	62.97468423309537	-26.90510021282638	-1.63870507642905
69(H)	65.19583439746117	-27.96343302444556	-1.37225880380760

Table S5. Cartesian coordinates for triplet H_3**TPTB**.

Atomic space	**x**	**y**	**z**
1(C)	66.65744266061141	-29.02036919727405	0.84616065021297
2(C)	66.75772979388269	-30.44056857056021	0.89893894981697
3(C)	68.02543312964664	-31.04554491442761	0.74621534456611
4(C)	69.15083292230572	-30.24301700118628	0.34883281865215
5(C)	68.86338625432278	-28.94271186535201	-0.25613016847492
6(C)	67.60865922816110	-28.32291268864718	-0.01818530436220
7(C)	68.23241730773978	-32.40604516920131	1.09483011580910
8(C)	69.49767553946542	-32.93515782835991	1.12946578162328
9(C)	70.59792187516621	-32.11917352524688	0.86869741880037
10(C)	70.44710351515808	-30.78027131999704	0.49958328317401
11(C)	69.75844293648085	-28.33976899794827	-1.15282027410803
12(C)	69.46188937243186	-27.13627572062711	-1.75458436195121
13(C)	68.23441927264511	-26.52773295353909	-1.51850588273914
14(C)	67.28940030076234	-27.11495716932489	-0.68447068937681
15(C)	65.74522106270699	-28.40834352212032	1.68730967250372
16(C)	64.88584537351169	-29.19264977844274	2.53732874284754
17(C)	64.77679742277746	-30.53141363691326	2.37525260636504
18(C)	65.53630834843186	-31.17405459235695	1.31938142795276
19(C)	65.02959625239203	-32.25703549258867	0.57333000864553
20(C)	71.70316611705424	-29.99112745414380	0.40865993256896
21(C)	65.95147053004484	-26.47408282661788	-0.62667971565112

22(C)	63.85947418301366	-32.97148486737219	0.97476965284224
23(C)	63.36498668714726	-34.01214657060002	0.23015793390576
24(C)	63.97858056565337	-34.40149037812048	-0.97675330742762
25(C)	65.11822880586101	-33.69809152743994	-1.39883323633534
26(C)	65.63583506118708	-32.66991837085906	-0.65473299828621
27(C)	72.78729546932510	-30.46409509141643	-0.33625912763435
28(C)	74.00120984996433	-29.79426412088291	-0.33625970651600
29(C)	74.16222147578628	-28.64002929496573	0.42945473887846
30(C)	73.08232899623052	-28.15726513376964	1.17360702705969
31(C)	71.86847457200557	-28.81833434621199	1.15478452143214
32(C)	65.84185670693257	-25.11333510314035	-0.33425911143546
33(C)	64.60690675116858	-24.48382498634717	-0.31341504265663
34(C)	63.44948253788262	-25.21240971395772	-0.58225247169616
35(C)	63.55110630948135	-26.56906258642932	-0.89940692418518
36(C)	64.78529308041637	-27.18982414600200	-0.92495507006878
37(C)	63.45844675884741	-35.46816711370838	-1.86783495879836
38(C)	75.45380465610893	-27.91715200222686	0.51420487989917
39(C)	62.10305254699939	-24.59852063065020	-0.53487701418170
40(O)	76.36904202987695	-28.34404901529426	-0.39440985385827
41(H)	77.16896747345685	-27.81856098280596	-0.23721042967605
42(O)	75.70153821859620	-27.03807799091184	1.30497969656600
43(O)	61.06397777960013	-25.19067041529413	-0.70840858086104
44(O)	62.13456232027004	-23.26752116124265	-0.26311955609225
45(H)	61.21011902938328	-22.97451339988191	-0.25115935127111
46(O)	62.51529970160398	-36.30752905763996	-1.35572830934691
47(O)	63.81676435507607	-35.61080190461547	-3.00912889174325
48(H)	62.41412756572579	-36.16343551015371	-0.40664411596016
49(H)	67.38565809293308	-33.01088181561487	1.37719931750935
50(H)	69.64815580949676	-33.96779638225519	1.41581551769649
51(H)	71.59722895422030	-32.51442179680033	0.99268066819087
52(H)	70.68459036921774	-28.83286021699278	-1.39757046269752
53(H)	70.16569336808377	-26.68704620176495	-2.44282913088633
54(H)	67.97717758012796	-25.61464339109914	-2.03826182223965
55(H)	65.71561459187861	-27.33301457783203	1.77244505544353
56(H)	64.28509087411123	-28.68357019019936	3.27933398697163
57(H)	64.06680916834898	-31.09411005726686	2.96484776353406
58(H)	63.34455622344157	-32.68915288638999	1.88067989219431
59(H)	62.45736902587004	-34.49353782457786	0.57571433105770
60(H)	65.57145808663560	-33.98264324763076	-2.33798625184221
61(H)	66.50450422667839	-32.14326626668777	-1.01627981943585
62(H)	72.67299810268757	-31.36322911043312	-0.92684703352027
63(H)	74.82953183041077	-30.17227265488046	-0.91838461900287
64(H)	73.21899471454329	-27.26603140967584	1.76998048505632

65(H)	71.03825420265555	-28.43677935869222	1.73345106424087
66(H)	66.73515316329126	-24.54866117541848	-0.10150895740547
67(H)	64.53574910700300	-23.43301533983879	-0.07295678030913
68(H)	62.64793449737035	-27.11912404609458	-1.12452212620466
69(H)	64.85321530768822	-28.23885240303589	-1.17745182777887

Table S6. The spin densities distribution of triplet H_3**TPTB**

Atomic space	Value	% of sum	% of sum abs
1(C)	-0.01	-0.75	-0.65
2(C)	0.26	**13.07**	**11.29**
3(C)	0.03	1.30	1.13
4(C)	0.10	4.91	4.24
5(C)	-0.01	-0.55	-0.48
6(C)	0.03	1.55	1.34
7(C)	0.10	5.18	4.47
8(C)	-0.02	-1.14	-0.99
9(C)	0.12	5.95	5.13
10(C)	-0.02	-1.00	-0.87
11(C)	0.02	0.87	0.75
12(C)	-0.01	-0.71	-0.62
13(C)	0.02	0.98	0.84
14(C)	-0.01	-0.62	-0.53
15(C)	0.27	**13.33**	**11.51**
16(C)	0.11	5.27	4.55
17(C)	0.10	5.07	4.38
18(C)	0.35	**17.36**	**14.99**
19(C)	0.05	2.66	2.29
20(C)	0.00	0.08	0.07
21(C)	0.00	0.23	0.20
22(C)	0.13	6.55	5.66
23(C)	-0.02	-0.90	-0.78
24(C)	0.17	8.52	7.35
25(C)	-0.02	-1.20	-1.04
26(C)	0.13	6.71	5.80
27(C)	0.00	-0.14	-0.12
28(C)	0.00	0.05	0.04
29(C)	0.00	-0.13	-0.11
30(C)	0.00	0.04	0.03
31(C)	0.00	-0.14	-0.12
32(C)	0.00	-0.12	-0.10
33(C)	0.00	0.17	0.15
34(C)	0.00	-0.10	-0.08

35(C)	0.00	0.22	0.19
36(C)	0.00	0.06	0.06
37(C)	0.02	1.02	0.88
38(C)	0.00	-0.02	-0.01
39(C)	0.00	-0.01	-0.01
40(O)	0.00	-0.01	-0.01
41(H)	0.00	0.00	0.00
42(O)	0.00	-0.04	-0.03
43(O)	0.00	-0.03	-0.03
44(O)	0.00	0.00	0.00
45(H)	0.00	0.00	0.00
46(O)	0.01	0.30	0.26
47(O)	0.05	2.63	2.27
48(H)	0.00	0.02	0.01
49(H)	0.01	0.52	0.45
50(H)	0.00	-0.08	-0.07
51(H)	0.01	0.42	0.36
52(H)	0.00	0.04	0.04
53(H)	0.00	-0.05	-0.04
54(H)	0.00	0.07	0.06
55(H)	0.02	0.81	0.70
56(H)	0.01	0.36	0.31
57(H)	0.01	0.50	0.43
58(H)	0.01	0.40	0.35
59(H)	0.00	-0.07	-0.06
60(H)	0.00	-0.08	-0.07
61(H)	0.01	0.56	0.48
62(H)	0.00	0.03	0.03
63(H)	0.00	0.00	0.00
64(H)	0.00	0.00	0.00
65(H)	0.00	0.01	0.01
66(H)	0.00	0.00	0.00
67(H)	0.00	0.01	0.01
68(H)	0.00	0.01	0.01
69(H)	0.00	0.05	0.04

Summing up above values: 2.00001300, Summing up absolute value of above values: 2.31628634

Table S7. The spin population distribution of H_3**TPTB**

Atom	Alpha pop.	Beta pop.	Spin pop.	Atomic charge
1(C)	3.02	3.04	-0.02	-0.07
2(C)	3.14	2.86	**0.28**	0.00
3(C)	3.04	3.02	0.02	-0.06

4(C)	3.05	2.95	0.10	-0.01
5(C)	3.02	3.03	-0.01	-0.05
6(C)	3.02	2.99	0.03	-0.01
7(C)	3.09	2.98	0.11	-0.08
8(C)	3.05	3.08	-0.03	-0.12
9(C)	3.11	2.97	0.13	-0.08
10(C)	3.02	3.04	-0.02	-0.05
11(C)	3.05	3.03	0.02	-0.07
12(C)	3.05	3.07	-0.02	-0.12
13(C)	3.05	3.03	0.02	-0.08
14(C)	3.02	3.03	-0.01	-0.05
15(C)	3.17	2.88	**0.29**	-0.06
16(C)	3.11	3.00	0.11	-0.12
17(C)	3.10	3.00	0.10	-0.10
18(C)	3.20	2.83	**0.37**	-0.02
19(C)	3.08	3.03	0.05	-0.10
20(C)	3.04	3.04	0.00	-0.09
21(C)	3.04	3.04	0.00	-0.08
22(C)	3.11	2.97	0.14	-0.08
23(C)	3.04	3.07	-0.03	-0.11
24(C)	3.14	2.97	0.18	-0.11
25(C)	3.02	3.05	-0.03	-0.07
26(C)	3.11	2.96	0.14	-0.07
27(C)	3.05	3.05	0.00	-0.10
28(C)	3.04	3.04	0.00	-0.08
29(C)	3.05	3.06	0.00	-0.11
30(C)	3.03	3.03	0.00	-0.06
31(C)	3.04	3.04	0.00	-0.08
32(C)	3.05	3.05	0.00	-0.10
33(C)	3.04	3.04	0.00	-0.08
34(C)	3.06	3.06	0.00	-0.11
35(C)	3.03	3.03	0.00	-0.06
36(C)	3.04	3.04	0.00	-0.08
37(C)	3.16	3.14	0.02	-0.30
38(C)	3.14	3.14	0.00	-0.28
39(C)	3.14	3.14	0.00	-0.28
40(O)	3.99	3.99	0.00	0.03
41(H)	0.41	0.41	0.00	0.19
42(O)	4.00	4.01	0.00	-0.01
43(O)	4.00	4.01	0.00	-0.01
44(O)	3.99	3.99	0.00	0.02
45(H)	0.41	0.41	0.00	0.19
46(O)	3.99	3.98	0.01	0.03

47(O)	4.02	3.97	0.05	0.01
48(H)	0.41	0.41	0.00	0.17
49(H)	0.43	0.43	0.00	0.15
50(H)	0.43	0.43	0.00	0.14
51(H)	0.43	0.43	0.00	0.14
52(H)	0.43	0.43	0.00	0.15
53(H)	0.43	0.43	0.00	0.14
54(H)	0.43	0.43	0.00	0.14
55(H)	0.43	0.43	0.00	0.14
56(H)	0.43	0.43	0.00	0.14
57(H)	0.43	0.43	0.00	0.13
58(H)	0.43	0.43	0.00	0.13
59(H)	0.44	0.44	0.00	0.13
60(H)	0.43	0.43	0.00	0.15
61(H)	0.43	0.43	0.00	0.15
62(H)	0.43	0.43	0.00	0.14
63(H)	0.43	0.43	0.00	0.14
64(H)	0.43	0.43	0.00	0.15
65(H)	0.43	0.43	0.00	0.14
66(H)	0.43	0.43	0.00	0.14
67(H)	0.43	0.43	0.00	0.14
68(H)	0.43	0.43	0.00	0.15
69(H)	0.43	0.43	0.00	0.14

Total net charge: 0.00000000, Total spin electrons: 2.00000000

Table S8. Spin natural orbital (SNO) contribution of triplet H_3**TPTB**

Atom	**SNO1 (%)**	**SNO2 (%)**
1(C)	1.72	3.98
2(C)	5.78	15.91
3(C)	2.85	3.37
4(C)	1.52	4.96
5(C)	0.25	0.78
6(C)	0.38	1.48
7(C)	1.70	5.02
8(C)	0.40	1.44
9(C)	1.72	5.86
10(C)	0.56	1.36
11(C)	0.18	0.42
12(C)	0.06	0.15
13(C)	0.21	0.52
14(C)	0.09	0.29
15(C)	5.72	15.07

16(C)	7.04	3.16
17(C)	4.10	5.72
18(C)	23.01	7.07
19(C)	4.40	5.10
20(C)	0.07	0.13
21(C)	0.07	0.27
22(C)	7.32	2.03
23(C)	2.16	1.25
24(C)	10.04	2.64
25(C)	2.10	1.00
26(C)	7.36	2.32
27(C)	0.05	0.06
28(C)	0.01	0.01
29(C)	0.03	0.00
30(C)	0.01	0.01
31(C)	0.04	0.05
32(C)	0.01	0.06
33(C)	0.03	0.13
34(C)	0.01	0.04
35(C)	0.05	0.21
36(C)	0.13	0.32
37(C)	2.07	0.99
38(C)	0.01	0.00
39(C)	0.00	0.01
40(O)	0.00	0.00
41(H)	0.00	0.00
42(O)	0.01	0.00
43(O)	0.00	0.00
44(O)	0.00	0.00
45(H)	0.00	0.00
46(O)	0.58	0.26
47(O)	2.46	0.87
48(H)	0.09	0.03
49(H)	0.36	0.76
50(H)	0.02	0.11
51(H)	0.16	0.65
52(H)	0.02	0.05
53(H)	0.00	0.01
54(H)	0.02	0.07
55(H)	0.48	1.47
56(H)	0.72	0.26
57(H)	0.31	0.83
58(H)	0.62	0.26

59(H)	0.12	0.13
60(H)	0.11	0.11
61(H)	0.57	0.67
62(H)	0.02	0.07
63(H)	0.00	0.00
64(H)	0.00	0.00
65(H)	0.01	0.05
66(H)	0.00	0.01
67(H)	0.00	0.01
68(H)	0.01	0.02
69(H)	0.04	0.14
Orbital delocalization index	9.31	7.43

Table S9 Composition of MO transition for calculated vertical transitions of singlet H_3**TPTB**[a]

excitation wavelength/nm (oscillator strength)	**composition of the excited-state wave functions**
203.49 (0.05816)	$0.37\ \Psi_{H-4\rightarrow L+5} + 0.08\ \Psi_{H-12\rightarrow L+2} + 0.05\ \Psi_{H-3\rightarrow L+5}$
204.36 (0.06591)	$0.56\ \Psi_{H-3\rightarrow L+5} + 0.09\ \Psi_{H-4\rightarrow L+5}$
214.8 (0.09362)	$0.21\ \Psi_{H-4\rightarrow L+4} + 0.15\ \Psi_{H-8\rightarrow L+1} + 0.12\ \Psi_{H-6\rightarrow L+4} + 0.08\ \Psi_{H-4\rightarrow L+3} + 0.05\ \Psi_{H-13\rightarrow L}$
215.18 (0.03252)	$0.21\ \Psi_{H-3\rightarrow L+4} + 0.14\ \Psi_{H-8\rightarrow L+1} + 0.13\ \Psi_{H-5\rightarrow L+3} + 0.09\ \Psi_{H-2\rightarrow L+8} + 0.08\ \Psi_{H-7\rightarrow L+2} + 0.06\ \Psi_{H-12\rightarrow L+1} + 0.06\ \Psi_{H-4\rightarrow L+4}$
215.62 (0.04866)	$0.38\ \Psi_{H-3\rightarrow L+4} + 0.08\ \Psi_{H-13\rightarrow L} + 0.06\ \Psi_{H-4\rightarrow L+3} + 0.06\ \Psi_{H-5\rightarrow L+3}$
216.19 (0.15324)	$0.27\ \Psi_{H-2\rightarrow L+8} + 0.14\ \Psi_{H-4\rightarrow L+3} + 0.14\ \Psi_{H-3\rightarrow L+4} + 0.08\ \Psi_{H-13\rightarrow L} + 0.06\ \Psi_{H-4\rightarrow L+4} + 0.05\ \Psi_{H-3\rightarrow L+3}$
217.33 (0.04994)	$0.2\ \Psi_{H-4\rightarrow L+3} + 0.18\ \Psi_{H-9\rightarrow L} + 0.11\ \Psi_{H-3\rightarrow L+3} + 0.08\ \Psi_{H-12\rightarrow L} + 0.07\ \Psi_{H-13\rightarrow L} + 0.06\ \Psi_{H-11\rightarrow L+1}$
218.86 (0.08057)	$0.17\ \Psi_{H-2\rightarrow L+7} + 0.15\ \Psi_{H-11\rightarrow L+1} + 0.1\ \Psi_{H-13\rightarrow L} + 0.06\ \Psi_{H-10\rightarrow L+1}$
221.24 (0.05517)	$0.23\ \Psi_{H-2\rightarrow L+7} + 0.15\ \Psi_{H-7\rightarrow L+2} + 0.08\ \Psi_{H-1\rightarrow L+7} + 0.05\ \Psi_{H-11\rightarrow L}$
223.68 (0.04208)	$0.72\ \Psi_{H-7\rightarrow L+1}$
225.84 (0.16302)	$0.25\ \Psi_{H-11\rightarrow L} + 0.14\ \Psi_{H-10\rightarrow L} + 0.11\ \Psi_{H\rightarrow L+8} + 0.07\ \Psi_{H-7\rightarrow L} + 0.07\ \Psi_{H-7\rightarrow L+2}$
231.01 (0.06644)	$0.44\ \Psi_{H-2\rightarrow L+6} + 0.21\ \Psi_{H-5\rightarrow L+1} + 0.05\ \Psi_{H-7\rightarrow L}$
231.23 (0.19189)	$0.33\ \Psi_{H-5\rightarrow L+1} + 0.25\ \Psi_{H-3\rightarrow L+2} + 0.13\ \Psi_{H\rightarrow L+8}$
232.53 (0.06993)	$0.36\ \Psi_{H-3\rightarrow L+2} + 0.17\ \Psi_{H-2\rightarrow L+6} + 0.13\ \Psi_{H-5\rightarrow L+1} + 0.06\ \Psi_{H-4\rightarrow L+2}$
232.79 (0.13938)	$0.41\ \Psi_{H\rightarrow L+7} + 0.34\ \Psi_{H-4\rightarrow L+2}$
233.58 (0.1251)	$0.39\ \Psi_{H\rightarrow L+7} + 0.25\ \Psi_{H-4\rightarrow L+2} + 0.08\ \Psi_{H-4\rightarrow L+1}$
236.39 (0.03266)	$0.49\ \Psi_{H-4\rightarrow L+1}$
239.07 (0.10222)	$0.41\ \Psi_{H-3\rightarrow L+1} + 0.22\ \Psi_{H-6\rightarrow L} + 0.05\ \Psi_{H-1\rightarrow L+4}$
239.77 (0.04673)	$0.4\ \Psi_{H-6\rightarrow L} + 0.27\ \Psi_{H-2\rightarrow L+5} + 0.12\ \Psi_{H-3\rightarrow L+1}$

247.08 (0.0365)	0.37 $\Psi_{H-3\rightarrow L}$ + 0.27 $\Psi_{H-4\rightarrow L}$ + 0.1 $\Psi_{H-3\rightarrow L+1}$ + 0.07 $\Psi_{H\rightarrow L+6}$
248.07 (0.07585)	0.22 $\Psi_{H-3\rightarrow L}$ + 0.17 $\Psi_{H-4\rightarrow L}$ + 0.09 $\Psi_{H-5\rightarrow L+2}$ + 0.08 $\Psi_{H-7\rightarrow L}$ + 0.06 $\Psi_{H-1\rightarrow L+5}$
251.8 (0.03268)	0.51 $\Psi_{H\rightarrow L+5}$ + 0.06 $\Psi_{H-4\rightarrow L}$ + 0.05 $\Psi_{H-2\rightarrow L+3}$
255.06 (0.03457)	0.35 $\Psi_{H-6\rightarrow L+1}$ + 0.08 $\Psi_{H-1\rightarrow L+5}$ + 0.07 $\Psi_{H-2\rightarrow L+7}$ + 0.05 $\Psi_{H-1\rightarrow L+7}$
259.11 (0.07905)	0.61 $\Psi_{H-2\rightarrow L+3}$ + 0.08 $\Psi_{H\rightarrow L+4}$ + 0.07 $\Psi_{H-1\rightarrow L+3}$
262.18 (0.08755)	0.59 $\Psi_{H-1\rightarrow L+4}$ + 0.08 $\Psi_{H\rightarrow L+3}$
263.52 (0.11929)	0.34 $\Psi_{H\rightarrow L+4}$ + 0.18 $\Psi_{H-1\rightarrow L+3}$ + 0.13 $\Psi_{H-2\rightarrow L+3}$ + 0.07 $\Psi_{H-7\rightarrow L}$
265.43 (0.04206)	0.21 $\Psi_{H-7\rightarrow L}$ + 0.16 $\Psi_{H-4\rightarrow L}$ + 0.11 $\Psi_{H-8\rightarrow L}$ + 0.1 $\Psi_{H-5\rightarrow L}$
291.45 (0.04914)	0.34 $\Psi_{H-2\rightarrow L+1}$ + 0.32 $\Psi_{H-1\rightarrow L+2}$ + 0.12 $\Psi_{H-1\rightarrow L+1}$ + 0.06 $\Psi_{H\rightarrow L}$ + 0.05 $\Psi_{H\rightarrow L+2}$
293.94 (0.14859)	0.3 $\Psi_{H-2\rightarrow L+1}$ + 0.27 $\Psi_{H-1\rightarrow L+2}$ + 0.19 $\Psi_{H\rightarrow L+1}$ + 0.1 $\Psi_{H-2\rightarrow L}$
301.81 (0.41399)	0.53 $\Psi_{H\rightarrow L+2}$ + 0.19 $\Psi_{H-1\rightarrow L+1}$ + 0.16 $\Psi_{H-1\rightarrow L+2}$ + 0.06 $\Psi_{H-2\rightarrow L+1}$
304.48 (0.1004)	0.28 $\Psi_{H\rightarrow L+1}$ + 0.23 $\Psi_{H-2\rightarrow L}$ + 0.2 $\Psi_{H-2\rightarrow L+1}$ + 0.1 $\Psi_{H-1\rightarrow L}$ + 0.09 $\Psi_{H-1\rightarrow L+2}$
307.04 (0.22812)	0.55 $\Psi_{H-1\rightarrow L+1}$ + 0.28 $\Psi_{H\rightarrow L+2}$
313.96 (0.12956)	0.61 $\Psi_{H-2\rightarrow L}$ + 0.19 $\Psi_{H\rightarrow L+1}$ + 0.06 $\Psi_{H-1\rightarrow L}$ + 0.05 $\Psi_{H\rightarrow L+2}$
325.93 (0.15005)	0.65 $\Psi_{H\rightarrow L}$ + 0.23 $\Psi_{H-1\rightarrow L}$

[a]Calculated Vertical Transition Energies ($\lambda > 200$ nm) for the Model Complexes from the TD-DFT Calculations (Excitations with oscillator strength $< 3 \times 10^{-2}$ are omitted, Only MO transitions with absolute contribution ≥ 5.0% are shown).

Table S10 Composition of MO transition for calculated vertical transitions of triplet H_3**TPTB**[a]

excitation wavelength/nm (oscillator strength)	**composition of the excited-state wave functions**
234.82 (0.06761)	0.17 $\Psi_{H\alpha-5\rightarrow L\alpha+1}$ + 0.05 $\Psi_{H\alpha-4\rightarrow L\alpha}$
235.67 (0.08836)	0.13 $\Psi_{H\beta-3\rightarrow L\beta+2}$ + 0.07 $\Psi_{H\beta-12\rightarrow L\beta+1}$ + 0.05 $\Psi_{H\alpha-5\rightarrow L\alpha+1}$
238.02 (0.04211)	0.15 $\Psi_{H\alpha-5\rightarrow L\alpha}$ + 0.11 $\Psi_{H\beta-3\rightarrow L\beta+2}$ + 0.08 $\Psi_{H\beta-2\rightarrow L\beta+2}$ + 0.07 $\Psi_{H\alpha-4\rightarrow L\alpha}$
239.17 (0.05918)	0.23 $\Psi_{H\beta-24\rightarrow L\beta}$ + 0.09 $\Psi_{H\beta-22\rightarrow L\beta}$ + 0.08 $\Psi_{H\beta-3\rightarrow L\beta+3}$ + 0.08 $\Psi_{H\alpha-5\rightarrow L\alpha}$
239.58 (0.07634)	0.18 $\Psi_{H\alpha-4\rightarrow L\alpha+1}$ + 0.1 $\Psi_{H\beta-2\rightarrow L\beta+3}$ + 0.09 $\Psi_{H\beta-24\rightarrow L\beta}$ + 0.06 $\Psi_{H\beta-23\rightarrow L\beta}$
242.58 (0.04898)	0.19 $\Psi_{H\beta-8\rightarrow L\beta+1}$ + 0.08 $\Psi_{H\beta\rightarrow L\beta+6}$
247.67 (0.037)	0.09 $\Psi_{H\alpha\rightarrow L\alpha+11}$ + 0.07 $\Psi_{H\alpha-8\rightarrow L\alpha+2}$ + 0.06 $\Psi_{H\alpha-8\rightarrow L\alpha+4}$
248.37 (0.05046)	0.08 $\Psi_{H\beta-2\rightarrow L\beta+2}$ + 0.07 $\Psi_{H\alpha-3\rightarrow L\alpha+3}$
250.98 (0.0304)	0.35 $\Psi_{H\beta-5\rightarrow L\beta+1}$ + 0.05 $\Psi_{H\alpha-1\rightarrow L\alpha+4}$
252.26 (0.0517)	0.18 $\Psi_{H\beta-5\rightarrow L\beta+1}$ + 0.07 $\Psi_{H\beta-10\rightarrow L\beta+2}$ + 0.06 $\Psi_{H\alpha-1\rightarrow L\alpha+4}$ + 0.05 $\Psi_{H\alpha-2\rightarrow L\alpha+3}$
252.82 (0.03651)	0.11 $\Psi_{H\beta-1\rightarrow L\beta+5}$ + 0.1 $\Psi_{H\alpha-2\rightarrow L\alpha+3}$ + 0.06 $\Psi_{H\alpha-4\rightarrow L\alpha}$
255.16 (0.04151)	0.08 $\Psi_{H\beta-10\rightarrow L\beta+2}$ + 0.06 $\Psi_{H\alpha-5\rightarrow L\alpha}$ + 0.06 $\Psi_{H\beta-1\rightarrow L\beta+4}$ + 0.05 $\Psi_{H\alpha-2\rightarrow L\alpha+3}$

256.11 (0.03319)	$0.3\ \Psi_{H\beta-4 \rightarrow L\beta+1} + 0.08\ \Psi_{H\beta-6 \rightarrow L\beta+1} + 0.07\ \Psi_{H\alpha-1 \rightarrow L\alpha+4}$
257.44 (0.04112)	$0.28\ \Psi_{H\alpha-1 \rightarrow L\alpha+5} + 0.13\ \Psi_{H\alpha-1 \rightarrow L\alpha+4}$
264.42 (0.05311)	$0.18\ \Psi_{H\alpha-2 \rightarrow L\alpha+2} + 0.09\ \Psi_{H\beta \rightarrow L\beta+5} + 0.08\ \Psi_{H\alpha-1 \rightarrow L\alpha+3} + 0.07\ \Psi_{H\alpha-1 \rightarrow L\alpha+4}$
281.85 (0.03127)	$0.21\ \Psi_{H\beta-7 \rightarrow L\beta+1} + 0.17\ \Psi_{H\alpha-1 \rightarrow L\alpha+2}$
283.98 (0.04362)	$0.14\ \Psi_{H\beta-1 \rightarrow L\beta+3} + 0.13\ \Psi_{H\alpha-3 \rightarrow L\alpha} + 0.06\ \Psi_{H\beta \rightarrow L\beta+4} + 0.06\ \Psi_{H\beta-1 \rightarrow L\beta+2} + 0.06\ \Psi_{H\alpha-2 \rightarrow L\alpha+1}$
289.07 (0.08923)	$0.12\ \Psi_{H\alpha \rightarrow L\alpha+10} + 0.12\ \Psi_{H\beta-1 \rightarrow L\beta+3} + 0.11\ \Psi_{H\alpha-2 \rightarrow L\alpha+1} + 0.09\ \Psi_{H\beta-6 \rightarrow L\beta+1} + 0.05\ \Psi_{H\alpha-1 \rightarrow L\alpha+2} + 0.05\ \Psi_{H\beta-17 \rightarrow L\beta}$
294.78 (0.05704)	$0.56\ \Psi_{H\beta-17 \rightarrow L\beta}$
297.04 (0.30967)	$0.28\ \Psi_{H\beta-1 \rightarrow L\beta+2} + 0.18\ \Psi_{H\alpha-3 \rightarrow L\alpha+1} + 0.08\ \Psi_{H\beta-1 \rightarrow L\beta+3} + 0.06\ \Psi_{H\alpha-2 \rightarrow L\alpha}$
299.26 (0.04425)	$0.15\ \Psi_{H\beta-4 \rightarrow L\beta+3} + 0.07\ \Psi_{H\alpha-5 \rightarrow L\alpha+1} + 0.07\ \Psi_{H\beta-1 \rightarrow L\beta+2} + 0.07\ \Psi_{H\alpha-6 \rightarrow L\alpha} + 0.07\ \Psi_{H\alpha-4 \rightarrow L\alpha+1}$
302.99 (0.10914)	$0.38\ \Psi_{H\beta \rightarrow L\beta+3} + 0.12\ \Psi_{H\alpha-2 \rightarrow L\alpha+1} + 0.09\ \Psi_{H\alpha-3 \rightarrow L\alpha} + 0.09\ \Psi_{H\alpha-1 \rightarrow L\alpha+1} + 0.08\ \Psi_{H\alpha-2 \rightarrow L\alpha}$
304.93 (0.03161)	$0.12\ \Psi_{H\alpha \rightarrow L\alpha+9} + 0.1\ \Psi_{H\alpha \rightarrow L\alpha+10} + 0.09\ \Psi_{H\alpha-3 \rightarrow L\alpha} + 0.07\ \Psi_{H\beta-1 \rightarrow L\beta+3} + 0.07\ \Psi_{H\beta-17 \rightarrow L\beta} + 0.05\ \Psi_{H\beta-2 \rightarrow L\beta+1}$
312.93 (0.03102)	$0.29\ \Psi_{H\beta-14 \rightarrow L\beta} + 0.1\ \Psi_{H\beta \rightarrow L\beta+2} + 0.06\ \Psi_{H\beta-13 \rightarrow L\beta}$
313.17 (0.03795)	$0.25\ \Psi_{H\beta \rightarrow L\beta+2} + 0.15\ \Psi_{H\alpha-1 \rightarrow L\alpha+1} + 0.1\ \Psi_{H\beta \rightarrow L\beta+3} + 0.09\ \Psi_{H\beta-14 \rightarrow L\beta}$
319.63 (0.05574)	$0.25\ \Psi_{H\alpha-1 \rightarrow L\alpha+1} + 0.09\ \Psi_{H\beta-2 \rightarrow L\beta+1} + 0.09\ \Psi_{H\alpha-1 \rightarrow L\alpha+2}$
326.62 (0.09384)	$0.26\ \Psi_{H\alpha-1 \rightarrow L\alpha} + 0.08\ \Psi_{H\alpha \rightarrow L\alpha+9} + 0.08\ \Psi_{H\alpha \rightarrow L\alpha+8} + 0.06\ \Psi_{H\alpha-3 \rightarrow L\alpha+1}$
335 (0.03413)	$0.21\ \Psi_{H\beta-1 \rightarrow L\beta+1} + 0.16\ \Psi_{H\alpha-1 \rightarrow L\alpha} + 0.12\ \Psi_{H\beta \rightarrow L\beta+2} + 0.09\ \Psi_{H\alpha-1 \rightarrow L\alpha+1} + 0.05\ \Psi_{H\beta-11 \rightarrow L\beta}$
383.61 (0.07116)	$0.26\ \Psi_{H\beta \rightarrow L\beta+1} + 0.18\ \Psi_{H\beta-12 \rightarrow L\beta} + 0.13\ \Psi_{H\alpha \rightarrow L\alpha+4}$
392.23 (0.04639)	$0.33\ \Psi_{H\beta \rightarrow L\beta+1} + 0.11\ \Psi_{H\beta-12 \rightarrow L\beta} + 0.08\ \Psi_{H\beta-13 \rightarrow L\beta} + 0.05\ \Psi_{H\alpha \rightarrow L\alpha+4}$
398.02 (0.06396)	$0.31\ \Psi_{H\beta-8 \rightarrow L\beta} + 0.16\ \Psi_{H\alpha \rightarrow L\alpha+4} + 0.06\ \Psi_{H\beta \rightarrow L\beta+1} + 0.05\ \Psi_{H\beta-3 \rightarrow L\beta}$
431.1 (0.03435)	$0.56\ \Psi_{H\beta-4 \rightarrow L\beta} + 0.2\ \Psi_{H\beta-6 \rightarrow L\beta} + 0.07\ \Psi_{H\alpha \rightarrow L\alpha+5}$
456.16 (0.03127)	$0.37\ \Psi_{H\alpha \rightarrow L\alpha+3} + 0.16\ \Psi_{H\beta-3 \rightarrow L\beta} + 0.15\ \Psi_{H\alpha \rightarrow L\alpha+4} + 0.12\ \Psi_{H\beta-7 \rightarrow L\beta}$
474.67 (0.1377)	$0.23\ \Psi_{H\beta-2 \rightarrow L\beta} + 0.18\ \Psi_{H\beta-3 \rightarrow L\beta} + 0.13\ \Psi_{H\alpha \rightarrow L\alpha+3} + 0.12\ \Psi_{H\beta-6 \rightarrow L\beta} + 0.08\ \Psi_{H\alpha \rightarrow L\alpha+2} + 0.07\ \Psi_{H\beta-4 \rightarrow L\beta} + 0.06\ \Psi_{H\beta-12 \rightarrow L\beta}$
512.33 (0.05551)	$0.38\ \Psi_{H\beta-2 \rightarrow L\beta} + 0.16\ \Psi_{H\alpha \rightarrow L\alpha+2} + 0.1\ \Psi_{H\alpha \rightarrow L\alpha+3} + 0.1\ \Psi_{H\beta-3 \rightarrow L\beta}$
711.73 (0.03829)	$0.55\ \Psi_{H\alpha \rightarrow L\alpha} + 0.15\ \Psi_{H\beta \rightarrow L\beta} + 0.13\ \Psi_{H\alpha \rightarrow L\alpha+1} + 0.09\ \Psi_{H\alpha \rightarrow L\alpha+2}$

[a]Calculated Vertical Transition Energies ($\lambda > 200$ nm) for the Model Complexes from the TD-DFT Calculations (Excitations with oscillator strength $< 3 \times 10^{-2}$ are omitted, Only MO transitions with absolute contribution ≥ 5.0% are shown).

Support References

[S1] Sheldrick, G. M. A Short History of SHELX. *Acta Crystallogr. Sect. A Found. Crystallogr.* **2008**, *64*, 112–122.

[S2] Sheldrick, G. M. Crystal Structure Refinement with SHELXL. *Acta Crystallogr. Sect. C Struct. Chem.* **2015**, *71*, 3–8.

[S3] Dolomanov, O. V.; Bourhis, L. J.; Gildea, R. J.; Howard, J. A. K.; Puschmann, H. OLEX2: A Complete Structure Solution, Refinement and Analysis Program. *J. Appl. Crystallogr.* **2009**, *42*, 339–341.

[S4] Grimme, S. Supramolecular Binding Thermodynamics by Dispersion-Corrected Density Functional Theory. *Chem. - A Eur. J.* **2012**, *18*, 9955–9964.

[S5] Neese, F. Software Update: The ORCA Program System, Version 4.0. *Wiley Interdiscip. Rev. Comput. Mol. Sci.* **2018**, *8*, 1–6.

[S6] Dorn, H. C.; Yannoni, C. S.; Limbach, H.-H.; Vogel, E., Evidence for a Nonclassical Structure of a 1,6-Methano[10]annulene: A Cryogenic ^{13}C CPMAS NMR Study of the 11,11-Dimethyl Derivative. *J. Phys. Chem.* **1994**, *98*, 11623–11627.

[S7] Weigend, F.; Ahlrichs, R. Balanced Basis Sets of Split Valence, Triple Zeta Valence and Quadruple Zeta Valence Quality for H to Rn: Design and Assessment of Accuracy. *Phys. Chem. Chem. Phys.* **2005**, *7*, 3297–3305.

[S8] Weigend, F. Accurate Coulomb-Fitting Basis Sets for H to Rn. *Phys. Chem. Chem. Phys.* **2006**, *8*, 1057–1065.

[S9] Lu, T.; Chen, F. Calculation of Molecular Orbital Composition. *Acta Chim. Sin.* **2011**, *69*, 2393–2406.

[S10] Lu, T.; Chen, F. Multiwfn: A Multifunctional Wavefunction Analyzer. *J. Comput. Chem.* **2012**, *33*, 580–592.

[S11] Risthaus, T.; Hansen, A., Grimme, S. Excited states using the simplified Tamm–Dancoff-Approach for range-separated hybrid density functionals: development and application. *Phys. Chem. Chem. Phys.* **2014**, *14*, 14408-14419.

[S12] Anouar H.; Weber F. Time-dependent density functional theory study of UV/vis spectra of natural styrylpyrones. *Spectrochimica Acta Part A*, **2015**, *115*, 675-682

[S13] Humphrey, W.; Dalke, A.; Schulten, K., VMD: Visual molecular dynamics. *J. Mol. Graphics* **1996,** *14*, 33-38.

[S14] Chen, G.; Sun, J.; Peng, Q.; Sun, Q.; Wang, G.; Cai, Y.; Gu, X.; Shuai, Z.; Tang, B. Z. Biradical-Featured Stable Organic-Small-Molecule Photothermal Materials for Highly Efficient Solar-Driven Water Evaporation. *Adv. Mater.* **2020**, *32*, 1–8.

[S15] Tan, Q.; Chen, H.; Xia, H.; Liu, B.; Xu, B. Parent and Trisubstituted Triazacoronenes: Synthesis, Crystal Structure and Physicochemical Properties. *Chem. Commun.* **2016**, *52*, 537–540.

[S16] Tan, Q.; Zhou, D.; Zhang, T.; Liu, B.; Xu, B. Iodine-Doped Sumanene and Its Application for the Synthesis of Chalcogenasumanenes and Silasumanenes. *Chem. Commun.* **2017**, *53*, 10279–10282.